



Review article

The current state of the art in internal additive materials and quantum dots for improving efficiency and stability against humidity in perovskite solar cells



Kanyanee Sanglee^a, Methawee Nukunudompanich^b, Florian Part^c, Christian Zafiu^c, Gianluca Bello^d, Eva-Kathrin Ehmoser^e, Surawut Chuangchote^{f,g,*}

^a Solar Photovoltaic Research Team, National Energy Technology Center, National Science and Technology Development Agency, 114 Thailand Science Park, Phaholyothin Road, Klong Nueng, Klong Luang, Pathum Thani 12120, Thailand

^b Department of Industrial Engineering, King Mongkut's Institute of Technology Ladkrabang (KMUTL), 1 Chalong Krung 1 Alley, Lat Krabang, Bangkok 10520, Thailand

^c Department of Water-Atmosphere-Environment, Institute of Waste Management and Circularity, University of Natural Resources and Life Sciences, Muthgasse 107, 1190 Vienna, Austria

^d Division of Pharmaceutical Technology and Biopharmaceutics, Department of Pharmaceutical Science, University of Vienna, Josef-Holaubek-Platz 2 UZA2, 1090 Vienna, Austria

^e Department of Nanobiotechnology, Institute for Synthetic Bioarchitectures, University of Natural Resources and Life Sciences, Muthgasse 11/II, 1190 Vienna, Austria

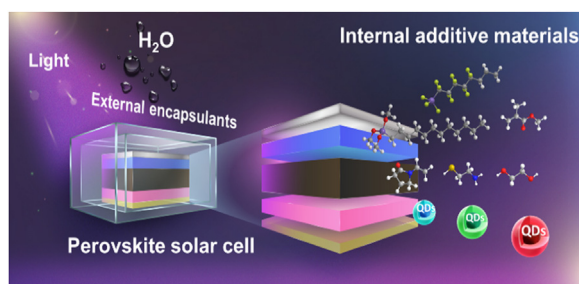
^f Department of Tool and Materials Engineering, Faculty of Engineering, King Mongkut's University of Technology Thonburi (KMUTT), 126 Prachauthit Rd., Bangmod, Tungkrui, Bangkok 10140, Thailand

^g Research Center of Advanced Materials for Energy and Environmental Technology (MEET), King Mongkut's University of Technology Thonburi (KMUTT), 126 Prachauthit Rd., Bangmod, Tungkrui, Bangkok 10140, Thailand

HIGHLIGHTS

- Surface passivation, polymer-mixed perovskite, and quantum dots (QDs) as strategies to enhance stability have been reviewed.
- QDs implemented in perovskite sheets, HTLs, and ETLs demonstrate improvements in the efficiency of perovskite solar cells.
- The implementation of QDs results in the reduction of recombination pathways, resulting in the long-term stability of devices.

GRAPHICAL ABSTRACT



ARTICLE INFO

Keywords:

Electron transporting layer
Hole transporting layer
Passivation
Perovskite solar cells
Quantum dots
Stability

ABSTRACT

The remarkable optoelectronic capabilities of perovskite structures enable the achievement of astonishingly high-power conversion efficiencies on the laboratory scale. However, a critical bottleneck of perovskite solar cells is their sensitivity to the surrounding humid environment affecting drastically their long-term stability. Internal additive materials together with surface passivation, polymer-mixed perovskite, and quantum dots, have been investigated as possible strategies to enhance device stability even in unfavorable conditions. Quantum dots (QDs) in perovskite solar cells enable power conversion efficiencies to approach 20%, making such solar cells competitive to silicon-based ones. This mini-review summarized the role of such QDs in the perovskite layer, hole-

* Corresponding author.

E-mail address: surawut.chu@kmutt.ac.th (S. Chuangchote).

<https://doi.org/10.1016/j.heliyon.2022.e11878>

Received 20 June 2022; Received in revised form 30 September 2022; Accepted 17 November 2022

2405-8440/© 2022 The Author(s). Published by Elsevier Ltd. This is an open access article under the CC BY-NC-ND license (<http://creativecommons.org/licenses/by-nc-nd/4.0/>).

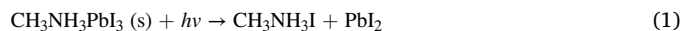
transporting layer (HTL), and electron-transporting layer (ETL), demonstrating the continuous improvement of device efficiencies.

1. Perovskite solar cells and their states of stability

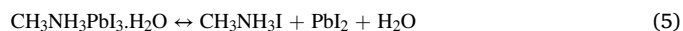
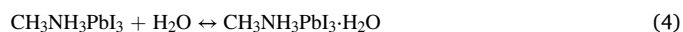
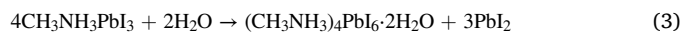
Photovoltaic (PV) devices, which are frequently called solar cells, harvest sunlight and convert it directly to electricity (as a renewable energy technology). For many years, silicon-based solar cells represent the industrial dominant standard technology in PVs. Such commercial technologies have historically been defined by their high performance, low cost, and stability. However, solar cells based on silicon are intrinsically compromised by high energy and material demand during production, and several difficulties with their end-of-life management, such as high costs to delaminate silicon wafers from the glass substrate or to recovery high-grade silicon (from mixed output materials after mechanical separation) by metallurgical processes [1, 2]. Emerging photovoltaics are on their way from lab-scale to industrial production [3]. Several researchers have identified perovskite solar cells, also named hybrid organic-inorganic perovskite solar cells, as particularly promising PV technologies alternatives [4, 5, 6]. These technologies not only demonstrate a high efficiency comparable to silicon-based solar cells, but also novel fields of application, as perovskite emerging photovoltaics can be designed of flexible, ultrathin, and light materials. Cost efficiency during the manufacturing processes can be improved by utilizing solution processes and simple fabrication methods at low temperature [7]. Thus, in comparison to silicon-based, energy, chemical, and material demand can be reduced by innovative (e.g., role-to-role) fabrication methods of perovskite solar cells [8]. Perovskite, a hybrid organic-inorganic material composed of halides with an ABX_3 crystal structure and polymeric substrates, is regarded as an ideal material for portable solar cell applications to deliver energy for off-grid solutions. Typically, perovskite cells are prepared by modifying one of two device configurations: the normal (n-i-p) or the inverted (p-i-n) configuration. Currently, the certified power conversion efficiency (PCE) of perovskite solar cells evolved from 3.8% in 2009 [4] to 25.5% in 2021 [9], but the long-term stability of the devices renders a significant barrier to successful commercialization [10]. An important technological leap in the development was made by the deposition of perovskite ($CH_3NH_3PbI_2Cl$) onto mesoporous Al_2O_3 and TiO_2 layers, which were contacted to 2,2',7,7'-tetrakis(N,N-di-p-methoxyphenylamine)-9,9'-spirobifluorene (spiro-MeOTAD) as hole transport layer (HTL) [11]. In 2021, Chen et al. [12], reported that dimethyl sulfoxide (DMSO), a liquid additive typically applied to enhance perovskite film morphology, was trapped during film formation. This leads to void formation at the interfaces of perovskite and substrate, accelerating the degradation of the film under illumination. The elimination of voids in the structure can be achieved by the replacement of dimethyl sulfoxide with carbonyldiimidazole. The obtained solar cells maintained high power conversion efficiency without efficiency loss of operation at 60 °C after 550 h. The validated PCEs of the perovskite mini-modules were 19.3% with an area of the aperture of 18.1 cm^2 [12].

Such novel solar cell architectures with organic-inorganic perovskite as a light-harvesting absorber thus possess a high absorption coefficient, excellent charge carrier mobility for electron-hole pairs, readily tunable bandgap energy, and a variety of facile synthetic processes for cell fabrication [13, 14, 15]. The general crystal structure of perovskite is ABX_3 , where A is an inorganic or organic cation that is larger than the metal cation B, and X represents the anion. The most frequently encountered hybrid perovskites are composed of methylammonium ($CH_3NH_3^+$), lead (Pb^{2+}), and a halide (I^- , Br^- , or Cl^-) or a mixture of halides [16, 17]. Probably the biggest disadvantage of perovskites is their instability under ambient environmental conditions, as these materials are sensitive to light, oxygen, and moisture [18, 19]. One of these

mechanisms is the photooxidation by the formation of superoxide free radicals ($O_2^{\cdot-}$) that are generated, when ammonium iodide (CH_3NH_3I) is illuminated and decomposes to water (H_2O), iodine (I_2), and methylamine (CH_3NH_2), while solid phases of PbI_2 remain as a product, as shown in Eqs. (1) and (2), respectively [18, 19]. Another possible photooxidation mechanism is initiated by the donation of an electron from the iodide anion (I^-), to oxygen molecules, resulting in the generation of superoxide free radicals that can cause damage to the perovskite.



Moisture also represents a significant impediment to the stability of perovskite solar cells. As shown in Eqs. (3), (4), and (5), moisture can trigger a different chemical reaction that leads to a structural change and consequently loss of photovoltaic efficiency [20, 21, 22]. Water molecules can degrade the perovskite structure of $CH_3NH_3PbI_3$ by the formation of octahedral lead iodide (PbI_6^{4-}) and PbI_2 (Eq. (3)). Another possible interaction of water molecules with $CH_3NH_3PbI_3$ is its initial integration, by an intermediate monohydrate ($CH_3NH_3PbI_3 \cdot H_2O$; Eq. (4)) that leads to degradation to CH_3NH_3I and PbI_2 with no phase separation (Eq. (5)).



It has been described [20, 21, 22] that lead iodide-based perovskite decomposes to PbI_2 when it is in contact with a polar solvent, such as water. There is still significant concern regarding the release of toxic lead into the environment, so lead-free perovskite composition must become the standard for environmentally friendly solar cell technologies [23]. Thus, strategies for preventing environmental factors, particularly moisture, reacting with perovskite materials in photovoltaic cells include (i) encapsulation of such devices as an external protection measure and (ii) passivation engineering as internal protection approach.

This review focuses on strategies for improving the stability and efficiency due to internal protection by using additives for material passivation, which includes surface perovskite films, large- and small-molecule additives, and quantum dots (QDs) additives. By avoiding the decomposition of perovskite materials, the release of toxic materials such as Pb compounds can be reduced, which can turn perovskite-based cells into good candidates for the development of more sustainable solar cells. This work also discusses the fundamental theory and unique properties of QDs. Here we want also to highlight the various types of QDs (and their exceptional photonic properties) that can be integrated into the active layer, hole-transporting layer (HTL), and electron-transporting layer (ETL) of perovskite photovoltaic devices and could improve these technologies to become more sustainable and efficient.

2. Challenges in stabilizing perovskite solar cells

Uniform perovskite films degrade rapidly when they are subjected to environmental factors such as heat, moisture, light, and radiolysis. Moisture leads to structural defects, as perovskite is very hygroscopic [24]. UV light leads to photodegradation of the perovskite or TiO_2 layers. Oxidation and formation of large PbI_2 structures can also occur, especially at high temperatures and in humid environments [25]. Some research groups have investigated perovskite films with high moisture sensitivity by studying color-changing perovskite films in atmospheric

moisture [26, 27, 28]. As previously addressed, moisture stability represents a major obstacle to the commercialization of perovskite solar cells. Perovskite films degrade rapidly in the presence of water and oxygen, where water molecules quickly form strong hydrogen bonds, which form hydroiodic acid (HI) [28]. Imperfections, such as bulk flaws, grain boundaries, surface flaws, and interface flaws are usually the places where the degradation is initiated [29, 30]. Generally, preparation methods for metal halide perovskite films that are based on wet chemistry reduce the performance of the final solar cell device [30]. Defects in the perovskite solar cells have also an impact on the efficiency leading to voltage losses and weak charge transport, both of which are caused by the formation of undesirable non-radiative channels. Photo-generated charge carriers recombination occurs through such non-radiative channels, adversely affecting the efficiency of perovskite solar cells [29, 30]. As a result, it is essential to develop hydrophobic materials that can ideally prevent the diffusion of moisture to the perovskite, passivate defects, and promotes charge transport.

3. Improvement of humidity stability in perovskite solar cells

3.1. External encapsulation of perovskite solar cells

The simplest solution to prevent the diffusion of moisture into photovoltaic cells is a tight encapsulation. More common device encapsulation methods typically include the use of appropriately sized glass coverslips, which can be applied to the entire device based on rigid substrates [31], and can then be sealed with epoxy resin, surlyn, ethylene vinyl acetate (EVA) as well as polyolefin materials for the laboratory manufacturing process. When working in small production scales, this encapsulation technique might be acceptable but is currently impractical for larger-scale productions [7, 32, 33].

3.2. Modification of perovskite films by surface passivation

To protect the surface from moisture, one strategy is to incorporate a thin passivation layer. Incorporating a thin insulating contact layer between the perovskite/cathode sides resulted in a straightforward method of preventing water-induced damage. The ultra-thin insulating layer inserted into the perovskite film enables charge tunneling, which not only transfers electrons from the perovskite film to the HTL but also blocks holes at the interface, as illustrated in Figure 1a [34]. The insulating layer needs to be as thin as possible, but sufficiently thick to withstand moisture. The critical tunneling properties of the insulation layer have been discussed and summarized in previous review reports [35, 36]. As shown in Table 1, a variety of polymeric insulating materials and insulating oxides (such as Al_2O_3) were reported to improve moisture protection in perovskite solar cells.

The majority of these materials consist of alkyl chains, acids, and thiol groups. By coating on top of the perovskite surface, the hydrophilic nature of the perovskite film is altered, resulting in the formation of hydrophobic films. For example, Zhang et al. used amphiphilic dodecyl-trimethoxysilane (C_{12} -silane) as an insulating layer with an alkyl chain to passivate the perovskite/HTL interface (Figure 1b). They discovered that the hydrophobic alkyl chain layer created a more resistant perovskite surface, as the contact angle of perovskite with C_{12} -silane was increased from 44.1° to 86.3° in the reference films [37].

Following that, Xiong et al. reported that using 2%wt triethoxy-1H,1H,2H,2H-tridecafluoro-*n*-octylsilane- $(\text{C}_{13}$ -FAS) as a fluoroalkyl silane for perovskite surface encapsulation reduced the device hysteresis and improved the stability in air at ca. 50% humidity [38]. The efficiency of perovskite solar cells covered by C_{13} -FAS through spin coating remained at 12% humidity for 500 h, when compared to a non-coated cell that was operated at 1% humidity for 250 h. Additionally, the contact angle as a measure for hydrophobicity of the unmodified perovskite surface was around 41.8° , whereas the C_{13} -FAS modified perovskite film

presented a maximum contact angle of 85.5° (Figure 1c). As a result, both C_{12} -silane and C_{13} -FAS contain a silanol (Si-OH) group that can be absorbed onto the perovskite surface via a hydrogen bond between the Si-OH and the perovskite iodide ion [38]. Zhu et al., found that surface modification of $\text{CH}_3\text{NH}_3\text{PbI}_3$ with 4-dimethylaminobenzoic acid (4-DMABA) increased the stability of the material up to 1000 h at 70% relative humidity and additionally the efficiency of perovskite photovoltaic applications from 17.43% to 19.87% [39]. The concept beyond 4-DMABA films is that its carboxyl group coordinates closely with lead (Pb^{2+}) in perovskite crystals, while the hydrophobic properties of the ligand are effectively repelling water molecules. Figure 1d illustrates the interaction mode of 4-DMABA molecules with MAPbI_3 [39]. Cao et al., calculated the effect of covering perovskite films with pentafluorobenzenethiol (e.g., $\text{HS-C}_6\text{F}_5$) on the hydrophobic thiol molecule layer through the Pb-S bonding interaction [40]. Similarly, Abdelmageed et al., investigated the use of a spin coating to deposit oleic acid (OA) on top of perovskite layers, resulting in the formation of hydrophobic thin films through the interaction of the OA carboxyl group (COO^-) with the Pb^{2+} and/or CH_3NH_3^+ ion groups. This modification demonstrated that the sample could remain stable at 76% humidity for four weeks [41]. Another way to improve the stability of photovoltaic cells was to deposit Al_2O_3 , which serves as a surface passivation layer between the perovskite/HTL interface, by atomic layer deposition, maintaining the efficiency of the cell for approximately 1680 h at 40–70% relative humidity, as measured by Koushik et al. [42].

Many research reports have continuously improved the stability of inverted perovskite solar cells against high humidity by using polymer additives in different layers of perovskite solar cells [43, 44, 45, 46, 47, 48]. Zhang et al. optimized HTL with polyphenylene sulfide as insulating additives, thereby increasing PCE from 19.1 to 21.5 % and achieving 574 h of device stability under aging conditions. The improvement is due to the larger grain sizes of perovskite film and optimized energy-level alignment at the interface between HTL/perovskite after the addition of polyphenylene sulfide, which suppresses the additive-induced decrease in conductivity [43]. Using polymer additives such as a fluorinated lead salt in a methylammonium lead iodide perovskite composition transforms the perovskite layer into the three-dimensional methylammonium lead iodide perovskite, allowing the fabrication of simple inverted solar cells at low temperatures [44]. Additionally, there are several polymer additives for using in the inverted structure like polyaniline-modified camphor sulfonic acid (PANI-CSA) in HTL [45], using a novel ionic silicone polymer in perovskite layer to chelate undercoordinated Pb^{2+} and Pb clusters to passivate deep defect [46] and also using the mixed polymer made of an indacenodithiophene and a thiadiazolequinoxaline (PIDTTDQ) replace PEDOT:PSS as a new hydrophobic HTL [47], and another by inducing amine-functionalized small molecules between ETL/electrode [48]. Thus, additive engineering is an effective strategy as a simple technique with enhanced solar cell stability of inverted perovskite solar cells.

In summary, a simple method to protect perovskite from moisture is to cover it with hydrophobic ultra-thin films on top of the perovskite surface by solution processes or vapor-deposition methods, as shown in the above-mentioned approaches. For such coatings, small organic molecules were shown to perform well, when they contained amphiphilic or hydrophobic groups. Several hydrophobic molecules can be employed to increase the stability of the nano-interfaces of perovskite surfaces in conditions of relative humidity ranging between 45% and 75%, which are summarized in Table 1.

3.3. Modifications of perovskite films by additive materials

3.3.1. Polymeric additives in perovskite precursors

Due to the high hygroscopicity of perovskite, additives with small and large molecules in perovskite precursors are regarded as a promising way to increase the stability of perovskite solar cells [22]. Figure 2 illustrates

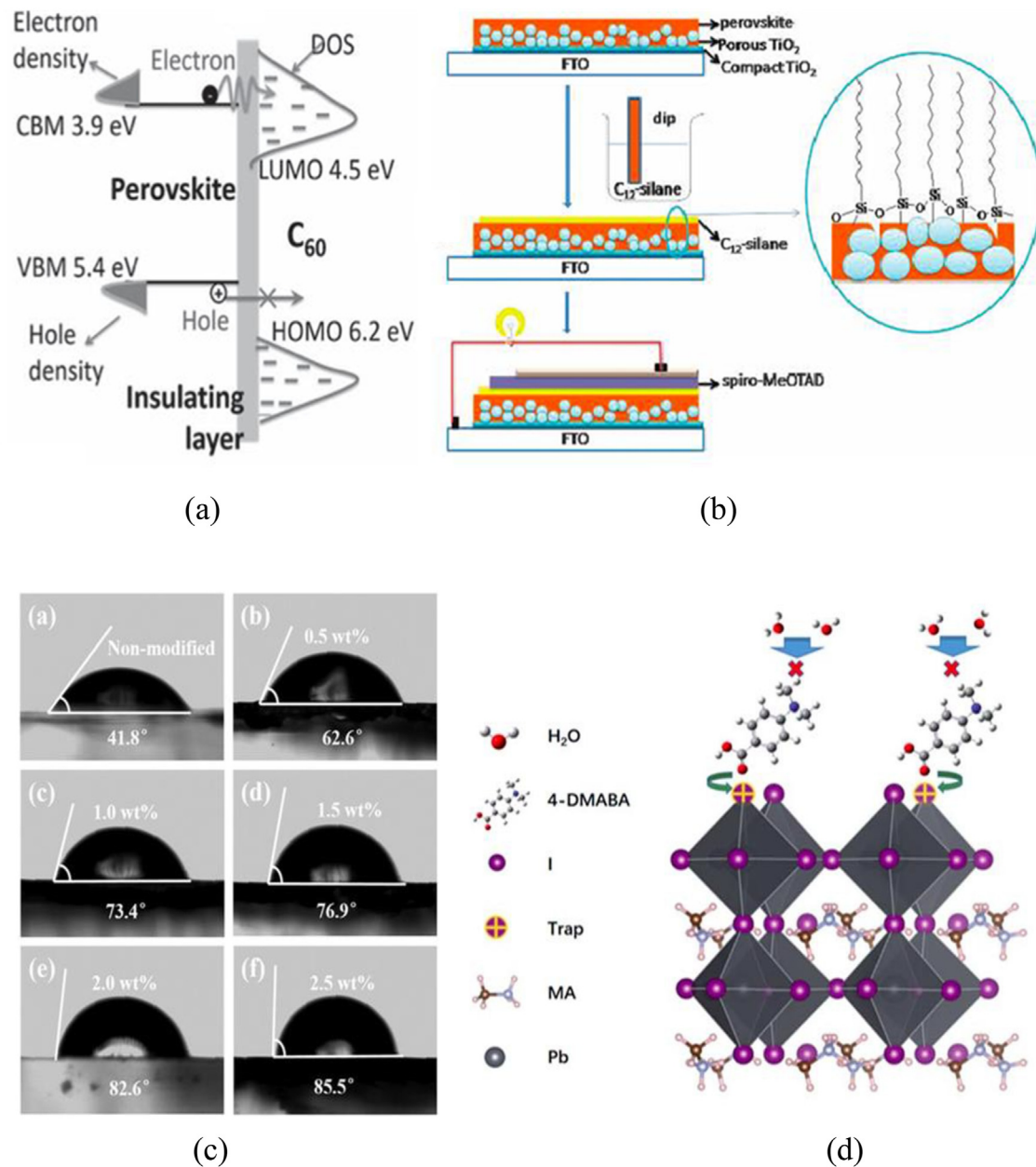


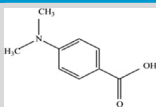
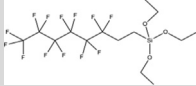
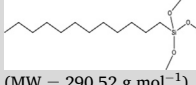
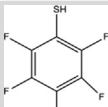

Figure 1. a) The energy diagram illustrates the principle of suppressing surface charge recombination by the insulating layer strategy. The insulating layer of choice suppresses charge recombination by separating the excess electrons and holes in the electron transport layer and perovskite layer, respectively (reproduced with permission [34], copyright 2016, Wiley Online Library); b) The formation process of the mesoporous perovskite device with C_{12} -silane modification (reproduced with permission [37], copyright 2015, The Royal Society of Chemistry); c) The contact angle of unmodified and modified perovskite film of C_{13} -FAS (reproduced with permission [38], copyright 2016, The Royal Society of Chemistry); and d) Schematic diagram showing the interaction mode of 4-DMABA molecules with $MAPbI_3$ (reproduced with permission [39], copyright 2018, The Royal Society of Chemistry).

the chemical structures of various additive materials in perovskite solutions while Table 2 summarizes several known polymeric additives for perovskite modifications. The illumination of perovskite films in presence of oxygen leads to its degradation and to the formation of structural defects in the nanocrystals and in turn to a decrease of the PCE [49, 50]. According to the degradation mechanisms, superoxide (O_2^-) is formed when oxygen (O_2) reacts during UV exposure to perovskite films. When O_2 reacts with the perovskite surface, methylamine (CH_3NH_2), PbI_2 , water, and I_2 are generated and thus inhibit the crystallization of the perovskite structure during particle growth or the deposition methods to

fabricate the layers. Polymer-additives can inhibit the diffusion of O_2 and maintain the perovskite crystallization when they are added to a perovskite precursor solution.

Xiang et al. [51] synthesized poly(dimethylsiloxane)-urea (PDMS-urea), the co-block polymer, which was used to fabricate perovskite solar cells. They discovered that PDMS-urea significantly improved the stability of perovskite solar cells because a portion of the urea group could form tight hydrogen bonds with the perovskite while the poly(dimethylsiloxane) domains provided a flexible, hydrophobic chain that protected the light-absorber surface from moisture.

Table 1. Various passivation layers increase the humidity stability of perovskite absorbers.

Passivation layer	Chemical structure (Molecular weight, MW)	Material property	Device stability/humidity test	Contact angle of perovskite films	Ref.
4-dimethyl aminobenzoic acid	 (MW = 165.19 g mol ⁻¹)	Hydrophobic	1,000 h, 70 %RH	65.0° (with passivation layers) – 45.0° (without passivation layers)	[39]
Triethoxy-1H,1H,2H,2H-tridecafluoro-n-octylsilane (C ₁₃ -FAS)	 (MW = 510.37 g mol ⁻¹)	Hydrophobic	500 h, ~50 %RH	85.5° (with passivation layers) – 41.8° (without passivation layers)	[38]
Dodecyl-trimethoxysilane (C ₁₂ -silane)	 (MW = 290.52 g mol ⁻¹)	Amphiphilic	600 h, 45 %RH	86.3° (with passivation layers) – 44.1° (without passivation layers)	[37]
Pentafluorobenzen ethiol	 (MW = 252.20 g mol ⁻¹)	Hydrophobic	250 h, 45 %RH	-	[40]
Oleic acid (OA)	 (MW = 282.47 g mol ⁻¹)	Hydrophobic	672 h, ~76 %RH	-	[41]
Aluminum oxide	Al ₂ O ₃ (MW = 101.96 g mol ⁻¹)	Insoluble in water	1,680 h, 40-70 %RH	-	[42]

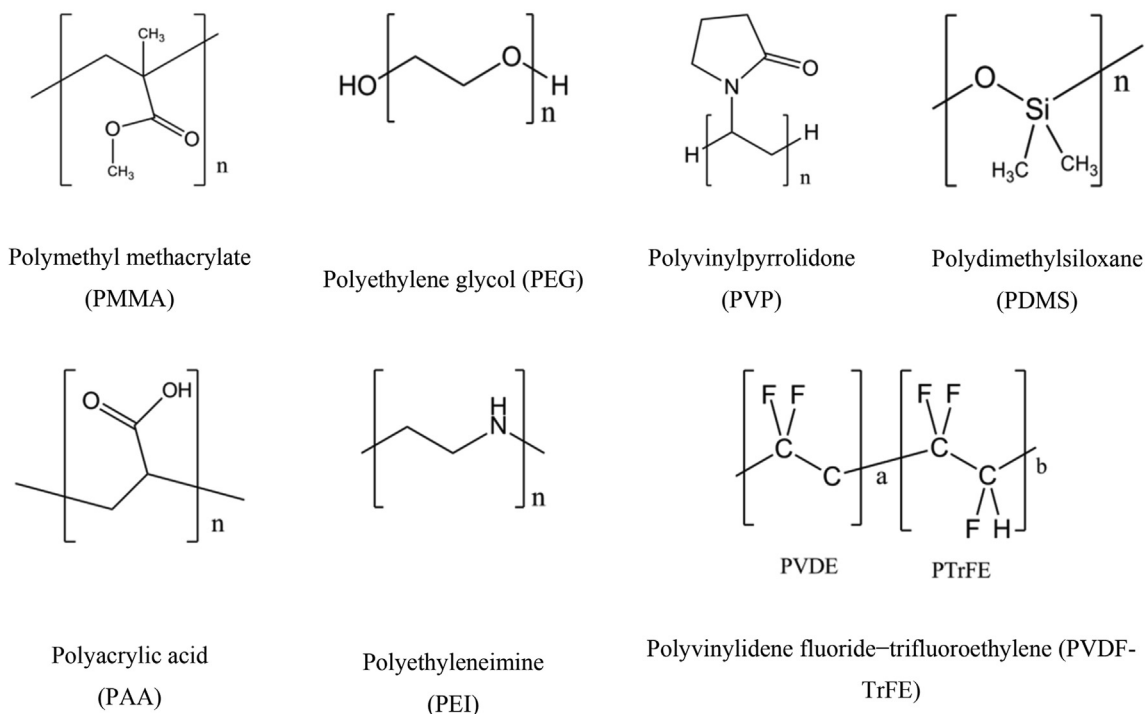
Internal encapsulating perovskite solar cell devices with polymethyl methacrylate (PMMA) represents a standard procedure for increasing stability against humidity. The PMMA was used to enhance nucleation and improve the uniformity of the perovskite films with high charge transfer properties. A combination of perovskite and PMMA for surface passivation of the absorber layer demonstrated a certified PCE of over 21% from Bi et al. [52] Zhao et al. [53] recorded on a uniform perovskite film with a polyethylene glycol (PEG)-scaffold model with a PCE of 16%. After 300 h of aging at 70% relative humidity, the unencapsulated perovskite solar cell retained 65% of its PCE. In Figure 3a, a schematic diagram illustrating the fabrication process of a perovskite film with a PEG scaffold using a one-step spin coating method is shown, along with SEM images of the perovskite surface without and with PEG. This work demonstrated the self-healing properties of PEG-scaffold perovskite films due to the PEG molecules with high hygroscopicity, which can form hydrogen bonds with the methylammonium iodide (MAI) molecules in perovskite [53]. Sun et al. published the use of polyvinylidene fluoride trifluoroethylene P(VDF-TrFE) as an additive polymer in PbI₂ solution to boost the photovoltaic efficiency of devices through a two-step deposition process [54]. The addition of the polymer P(VDF-TrFE) raised the PCE from 9.90% to 13.24% due to the improved crystallinity and morphology of the perovskite films caused by adding P(VDF-TrFE). Another study by Li et al., demonstrated that surface passivation, which was induced by polyvinylpyrrolidone (PVP), could aid the cubic phase formation of CsPbI₃ crystal structure and thus improving the long carrier diffusion length of perovskite. PVP was shown to adsorb physically onto the surface of CsPbI₃ and also form a coordinative bond that stabilized cubic CsPbI₃ through the acylamino group (N–C=O). PVP was coordinatively bound to the surface of CsPbI₃ crystals (Figure 3b) [55]. Another example was shown by Fairfield et al. [49], who investigated the effect of polymer additives such as polyethylene glycol (PEG), polyethyleneimine (PEI), poly(acrylic acid) (PAA), and polyvinylpyrrolidone (PVP) on the crystal sizes and stability of perovskite-polymer hybrid films

in humid air. Under humid air and illumination, it was discovered that perovskite–PAA hybrid solar cells retained a stable efficiency for the first three days and then gradually degraded over the next six days, while control perovskite solar cells degraded completely within the first two days (Figure 3c).

Polymer additives were used to extend the lifetime of perovskite. When these polymers were used, major improvements in perovskite dense films based on acid-base interaction were observed, as well as improved system stability under humid and illuminated conditions. There are many materials that were used as additives or passivation layers such as 3-aminopropyltrimethoxysilane [56], trichloro(octyl) silane [57], methoxysilane [58], poly(vinylidene fluoride-co-hexafluoropropylene) [59], polyamide [60], poly(styrene-co-acrylonitrile) polymer [61], polyvinyl butyral (PVB) [62], polyhedral oligomeric silsesquioxane-poly(trifluoroethyl methacrylate)-b-poly(methyl methacrylate) polymer [63], and both NbCl₅ and n-butylammonium bromide [64] in perovskite solar cells.

Apart from low-molecular-weight materials, Li et al. [65] reported the modification of the methylammonium lead triiodide (CH₃NH₃PbI₃) perovskite surface using a one-step spin coating method in the presence of 4-ABPACl. The benefit of using bifunctional 4-ABPACl molecules as additives is an increased moisture resistance by chemically anchoring ammonium (-NH₃⁺) cations, and phosphonic acids (-PO(OH)₂) and groups of the polymer to the perovskite grain surface through strong hydrogen bonding, that result in a photovoltaic performance from 8.8% to 16.7%. Also, 2-AET can be used as an additive and connect MAI and PbI₂ by a hydrogen bond between 2-AET and MAPbI₃. Additionally, Li et al. verified the stability of the mixed ligand-perovskite film by immersing it in water. The mixed film remained dark brown compared to pristine films, which was proven to the stability in the water. After DMF was removed, the thiolate groups of the ligand material may exhibit a stronger affinity for PbI₂, while the -NH₃⁺ group may exhibit affinity for MAI, forming PbI₂-2-AET- MAI [66].

Polymeric additive (large molecules)



Chemical additive (small molecules)

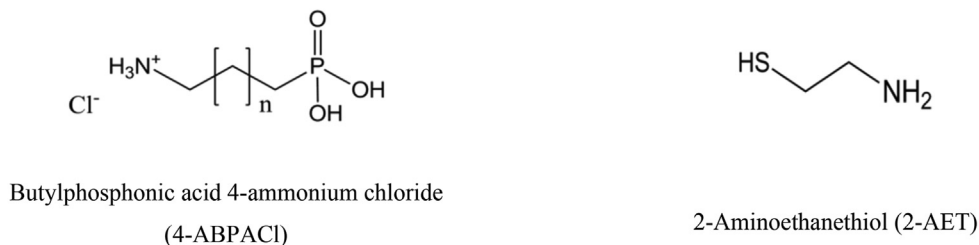


Figure 2. Chemical structures of large and small molecules additive materials for increasing the stability of perovskite.

3.3.2. Quantum dot (QD) additives

3.3.2.1. Fundamental theory of quantum dots and their stability-enhancing properties. Quantum dots (QDs) are semiconductor nanocrystals with tunable band gaps due to the quantum confinement effect, which have higher absorption coefficients than commonly used organic dyes, and multiple exciton generation [67, 68]. Over the last decade, QDs derived from II/VI and III/V semiconductors have matured into a new class of fluorescent markers for bioimaging probes, sensing, light-emitting, and optoelectronic applications. For example, colloidal quantum dots (CQDs) are favored due to their high photo- and thermal-stability in quantum dot solar cells [69, 70]. Quantum confinement offers an intriguing possibility for bandgap engineering. When particles are shrunk to less than their Bohr radius, the electron and hole wave functions are confined. Due to the wide bandgap, the optical transition exhibits a blue shift [71]. The quantum yield of photoluminescence or fluorescent quantum yield (Φ) is a critical performance indicator for determining the efficiency of QD fluorophores. Quantum yield values for photoluminescence represent the

ratio of emitted to absorbed photons [72, 73]. Normally, Φ can be estimated by comparing the absorbance and integrated fluorescence intensities of a single reference and unknown, using the following Eq. (6):

$$\Phi_x = \Phi_{std} \left(\frac{Grad_x}{Grad_{std}} \right) \left(\frac{\eta_x^2}{\eta_{std}^2} \right) \quad (6)$$

where Φ is the quantum yield of photoluminescence, $Grad$ is the gradient of the linear plot of integrated fluorescence intensity vs. absorbance, η is the reflective index of solvent, and the subscripts "x" and "std" denote the test sample and fluorescent standard, respectively [73].

Colloidal perovskite QDs have rapidly emerged as a new class of extraordinary nanocrystal semiconductors and have been extensively investigated for applications in other technical fields. Due to their superior photoluminescence efficiency, lead halide perovskite QDs are nearly as bright and narrow as those based on cadmium chalcogenide. The reasons for the varied perovskite compositions have been discussed in previous reviews for solar cells [74] and scintillators [75]. From CdTe-based polycrystalline solar cells, it is known that CdS nanocrystals are applied as the p-n junction with CdTe absorbers to increase the PCE

Table 2. Polymeric additives for perovskite modifications.

Type	Material	Molecular weight (g/mol)	Perovskite precursor	Step- deposition	Structure	PCE (%)	Testing condition: relative humidity and device stability	Ref.
Large-molecular	PDMS-Urea	850, 2500, 5000	MAPbI ₃	One-step	n-i-p	16.15	In dark with 50%RH, PDMS-urea (20 mg/ml) no degradation within 2500 h.	[53]
	PMMA	-	(FAI) _{0.81} (PbI ₂) _{0.85} (MAPbBr ₃) _{0.1}	One-step	n-i-p	21.00	3.3% decay in PCE during exposure to ambient air for two months in the dark.	[52]
	PEG, PEI, PAA, PVP	-	MAPbI ₃	One-step	p-i-n	16.00	Unsealed, 48% RH, retained initial PCE for 72 h.	[49]
	PEG	12,000, 20,000, 100,000	MAPbI ₃	One-step	n-i-p	16.00	-	[53]
	PVP	10,000	*CsPbI ₃	One-step	n-i-p	10.70	Under continuous light (10 h under 70 mW/cm ²) illumination, moisture for over 300 h.	[55]
Small-molecular	2-AET	77.15	MAPbI ₃	One-and two-step	-	-	-	[66]
	4-ABPACl	153.12	MAPbI ₃	One-step	n-i-p	16.70	In ambient air at ~55% RH in the dark, currently recorded at 10% illumination intensity, PCE remains at 14% for about a week.	[65]

* Cesium lead iodides (CsPbI₃), %Relative humidity (%RH).

owing to bandgap grading when S diffuses into the absorber material and thus extends the optical absorbance to shorter wavelengths due to CdTe_{1-x}S_x structures [3, 76]. In the following section, we will summarize and analyze the advantages of QDs in perovskite solar cells. MAPbBr₃, MAPbI_{3-x}Cl_x, or CsPbBr₃ QDs can be used embedded in bulk materials, as nanoparticles, or in form of nanoplates for perovskite polycrystalline thin films for solar cells [77] or light-emitting diodes (LEDs) [78, 79, 80, 81, 82] because of their high stability, facile structural, and photophysical tunability [83]. These QD types are typically referred to as perovskite QDs. Another colloidal form of these nanocrystals is chalcogenide QDs (e.g., CdS, CdSe, or CdTe) or lead halide QDs (PbS or MPbX). The latter QD type was applied to create CQD solar cells with a PCE of up to 10.6% [84]. Halide QDs can also be used for infrared-sensitive absorber materials and are therefore of interest in tandem solar cells [85]. Following the classification of solar cells by the National Renewable Energy Laboratory (NREL) [9], it must be highlighted that PbBr₃-like crystal structures are allocated to 'perovskite solar cells', while chalcogenide or halide CQDs are assigned to so-called 'quantum dot solar cells'.

Numerous recent studies demonstrated that QDs can be used to enhance the photon resistance stability and efficacy of hybrid organic-inorganic perovskites through effective charge separation following incident light absorption. Figure 4 shows the relationship between international publications collected and PCE of perovskite solar cells where QD materials have been integrated. The PCE increased from 3% [86] up to over 20% [87] in the period of 2014–2020. Thus, QDs are promising materials, which can be used to increase efficiency and commercialize perovskite solar cells.

QDs enhance the long-term photostability of perovskite photovoltaic devices (Table 3). The primary drawbacks of perovskite materials are their rapid degradation by moisture, their sensitivity toward UV light, and their electron-hole recombination. Thus, we emphasize the beneficial effect of QDs by stating that (i) some QDs were inserted between perovskite and TiO₂ layers, which can help to reduce the photocatalytic effect of TiO₂ that can damage the photoactive films [88], (ii) the most important QD species were passivated at the surface trap site of semiconductors, which prevented the formation of recombination pathways [89, 90], and (iii) most importantly, the introduction of QDs in

perovskite material, which can enhance material persistence around the VIS-NIR region due to light-induced degradation [91].

Over the last decade, CQDs have been synthesized as nanometer-scale semiconductor crystals capped with surfactant molecules and dispersed uniformly in solution. Controllability of the size and shape of QDs is important for tuning the quantum confinement effect, and optical and electrical properties, according to solution processing. All QD materials have shown exceptional efficiency in a wide variety of optoelectronic system groups. Generally, QD synthesis starts from small crystals that grow until the reaction is stopped. Two synthesis strategies that allow the controlled growth of QDs are widely used as illustrated in Figure 5. The in-situ process, which includes successive ionic layer adsorption and reaction (SILAR) and chemical bath deposition (CBD) [95], requires the growth direction of the QD self-assembly onto mesoporous substrates (e.g., metal oxide films). These reactions take place on electrode surfaces in the presence of a reactant precursor solution. For solar cell applications, ample QDs can be loaded into preferred metal oxide films (e.g., TiO₂ and ZnO) to allow for light harvesting while maintaining ease of preparation, and chemical stability [96, 97]. The QD-modified electrodes have a significant amount of sunlight harvesters and photoelectric conversion ability. Another ex-situ method is to prepare QDs by one-pot hydrothermal synthesis at temperatures between ca. 100–350 °C prior to their deposition on surface films with a known amount of QDs. Direct adsorption, electrophoretic deposition, and linker-assisted immobilization are the most frequently used methods for immobilizing the as-synthesized QDs on metal oxide semiconductor substrates. For the in- and ex-situ deposition designs that have been discussed previously [98, 99, 100].

We survey the synthesized QD routes in order to obtain high-quality QDs dispersed solid materials with ideal bandgap absorption and dispersion properties. The one-pot hydrothermal method is commonly used to provide colloidal QD nanocrystals with nano-size between 5–10 nm. The primary determinants of the size and shape of QD nucleation are temperature and supersaturation concentrations in solution [101, 102]. Surfactants or capping ligands are contained in the precursor solutions during synthesis to ensure that colloidal QDs have a high surface-to-volume ratio and increase colloidal stability and thus

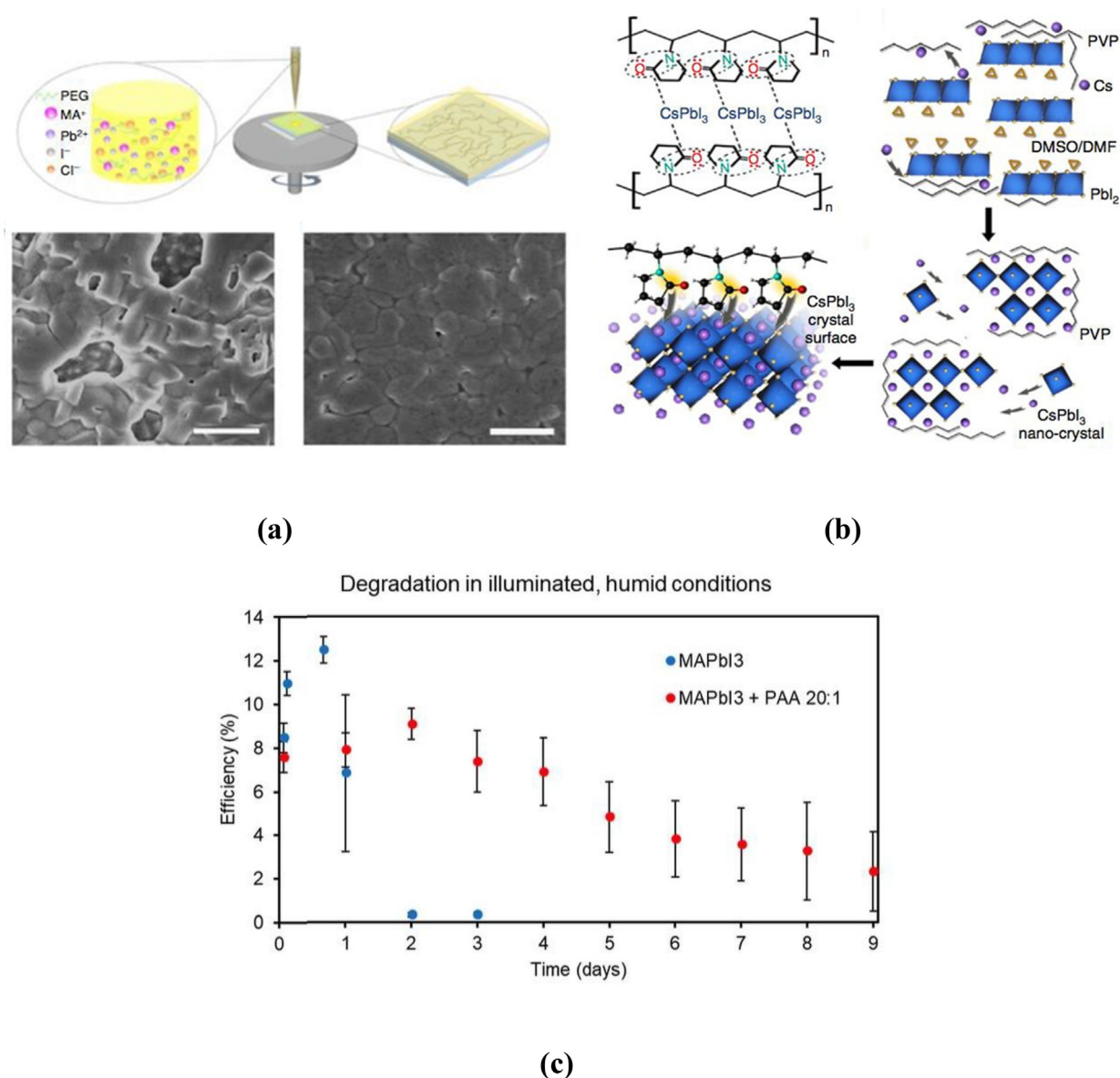


Figure 3. a) Schematic and SEM Image of perovskite surface without and with PEG via spin coating method (reproduced with permission [53], copyright 2016, Nature Communication); b) Chemical formation mechanism of PVP-induced cubic phase CsPbI₃ (reproduced with permission [55], copyright 2018, Nature Communication); and c) Stability of perovskite solar cell without and with PAA under 43% relative humidity in the air with illumination (reproduced with permission [49], copyright 2019, The Royal Society of Chemistry).

dispersibility. Typically, capping ligands have a polar head and a long hydrocarbon tail, such as trioctylphosphine oxide (TOPO), oleylamine, oleic acid (OA), 2-mercaptoethylamine (MA), and 1-octadecene (ODE). These ligands are chosen based on the Lewis values of acids and bases describing their reactivity in the precursor solution to coordinate chemistry with the QD surface atoms.

Numerous earlier studies have shown the use of various organic ligands such as fatty acids, long-chain amines, and phosphine acid groups as suitable ligands for controlling the structures and surface coordination of QDs. To obtain QDs with a narrow band distribution and shape, it is critical to select the appropriate ligands. For example, colloidal lead (Pb)- and cadmium (Cd)- chalcogenide QDs were synthesized in a hot-injection process under N₂/Ar conditions using PbO and/or CdO capped with oleic acid (Ol⁻, H⁺). This process resulted in the formation of Pb/Cd oleate, more precisely Pb/Ol and Cd-Ol quantum dots [103, 104]. Afterward, the respective reaction flask was rapidly filled with sulfur (S) and/or tellurium (Te) precursors to form the completed CQDs. Trioctylphosphine (TOP) and trioctylphosphine oxide (TOPO) ligand molecules capped

CdSe are primarily used for overcoating Cd atoms in a wet-chemical CdSe synthesis, as they have stronger capping properties than oleic acid [104, 105, 106, 107]. Due to their superior properties, colloidal QDs are promising materials for photovoltaics, light-emitting diodes, bioimaging, and drug delivery among other applications [108, 110, 111]. However, the instability of as-synthesized QDs is an obstacle to their further implementations and could result from the substitution of the ligands responsible for the instability. The modification of the surface of QDs by ligand exchange reaction can be done in solid-phase and solution-phase. Examples of ligand exchange are the replacement of pristine ligands (e.g., TOPO) with pyridine [104, 112]. Knauf et al. investigated the exchange of oleate-capped CdSe with phosphonic acids and thiols [113]. Reinhart and Johansson, compared the optical properties of as-synthesized 3-mercaptopropionic acid (3-MPA) capped PbS QDs to those of oleate-capped QDs [114].

3.3.2.2. Applications of quantum dots in perovskite solar cells. As illustrated in Table 4, we summarized different types of QDs for ETL,

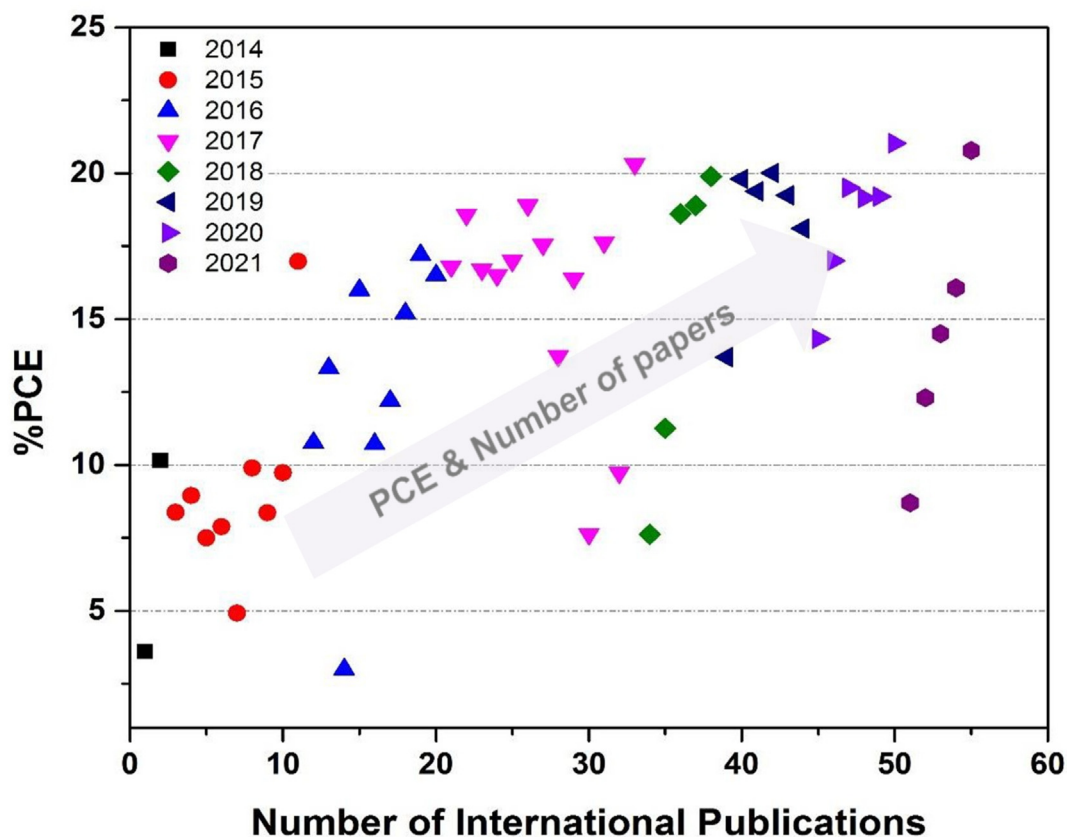


Figure 4. Improvement of QDs based perovskite solar cells as a function of the percentage power conversion efficiency (PCE%). Evaluated international journal articles that were published by The Royal Society of Chemistry, American Chemical Society, Nature Publishing Group, The Wiley Online Library, and Elsevier, etc., were searched by using the phrase “Quantum Dots for Perovskite Photovoltaic Devices”.

Table 3. Summary of the percentage degradation of perovskite solar cells (PSCs) with various QDs.

Perovskite solar cells	Time (h)	Initial-final efficiency (%)	Device degradation (%)	Ref.
PSCs	12	10.2–4.3	58.0	[89]
PSCs–CdS QDs		9.9–7.6	23.0	
PSCs	12	1.0–0.2	80.0	[91]
PSCs–Carbon QDs		1.0–0.7	30.0	
PCBM	70	11.2–7.0	37.5	[92]
PCBM–CdSe QDs		13.7–10.5	23.4	
CsPbI ₃	100	1.0–0.85	15.0	[93]
CsPbI ₃ –Mn QDs		1.0–0.98	2.0	
PSCs	97	1.0–0.3	70.0	[88]
PSCs–PbS QDs		1.0–0.8	20.0	
PSCs	720	8.5–1.0	90.0	[90]
PSCs–Graphene QDs		14.5–13.5	10.0	
PSCs	500	1.0–0.3	70.0	[94]
PSCs–CsPbBrCl ₂ QDs		1.0–0.8	20.0	

Designs of QD Synthesis Methods.

perovskite, and HTL layers in perovskite solar cells, demonstrating the parameters, namely a short current density (J_{sc}), an open-circuit voltage (V_{oc}), a fill factor (FF), and a percentage of power conversion efficiencies (PCE), for several cell compositions (measured at 1 sun-AM1.5G). Following sections will address QDs as an active layer in perovskite precursors, as well as HTLs and ETLs.

3.3.2.3. Quantum dots in perovskite layer. In general, the efficient performance strongly depends on the quality of perovskite active layers, such as their morphology, crystallinity, and composition. Therefore, a good crystal-forming process of the perovskite films, with high surface

coverage and minimum pinholes, is the most important factor that impacts the device performance. In turn, the main challenges to produce high-quality films are to control the crystal growth behavior, which depends on different factors such as the perovskite precursors, the deposition methods, the solvents, and the additives used [115, 116, 117, 118].

Some authors indicate that the instability of perovskite solar cells has not been resolved yet [119, 120]. Different QD types were used to produce QD perovskite solar cells. For example, cesium lead bromide QDs (CsPbBr₃) composited with mesoporous TiO₂ films have been synthesized and used to enhance electron transfer in photodetectors [121, 122]. In addition, the materials were also used to produce light-emitting diodes

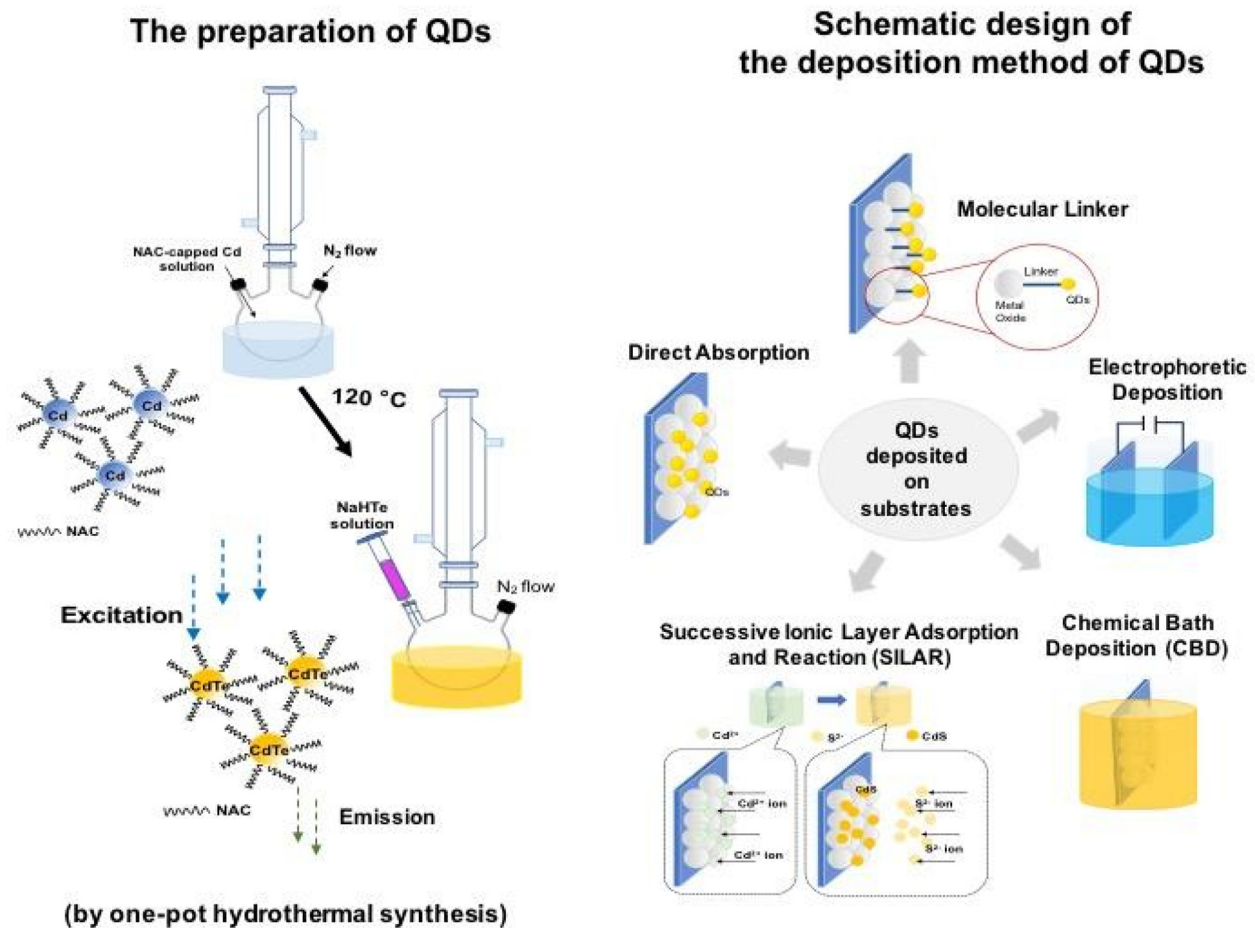


Figure 5. Possible designs (left) of QD one-pot hydrothermal synthesis of chalcogenic CdTe, CdSe, or CdS with short-chain linker molecules (e.g., N-acetyl-L-cysteine, NAC), which can be exchanged for other linker molecules of interest using thiol chemistry (SH bonding with the QDs of e.g. trioctylphosphine oxide, TOPO), and schematic design of QD-deposited on substrates (right).

(LEDs) [123, 124, 125] and lasers [126, 127]. Swarnkar et al. demonstrated that by synthesizing cesium lead iodide (CsPbI₃) QDs at temperatures ranging from 60 °C to 185 °C, they were able to monitor the QD size range of 3.4–12.5 nm, which corresponded to the shifted excitonic peaks of CsPbI₃ between 585 and 670 nm. Their ultraviolet (UV) emissions ranged from orange (585 nm) to red (670 nm), indicating an energy band difference of 2.07 to 1.82 eV. Laboratory scale perovskite devices demonstrated high efficiency of 10.77%, for which QDs in the size of 9 nm (synthesized at a temperature of 180 °C) were used [128]. Cha et al. proposed the fabrication of hybrid planar perovskite solar cells using synthesized MAPbBr_{3-x}I_x (MA = CH₃NH₃) QDs by varying the Br to I ratio. Their modified QDs (with an average diameter of 5 nm) were used as interface phases between the perovskite film and HTL; the best cell achieved a considerable PCE of 13.32% [129].

The concentration of tin sulfide (SnS) quantum dots (QDs) in methylammonium lead iodide (MAPbI₃) precursor solution was varied to improve carrier separation and transportation. The MAPbI₃/SnS QD hybrid structure can also be used as an absorber layer due to its PCE of 16.8%. Before centrifugation, a particle size of 3 and 6 nm of SnS QDs was determined [130]. The superior crystallization of hybrid perovskite films reveals a large grain size, which results in a PCE of up to 18.6% when lead sulfide (PbS) QDs are added to the MAPbI₃ precursor [131]. Also, graphene QDs were used during the perovskite solution process to overcome the grain boundaries effect of perovskite crystals on PSC performance by passivation. As a result, a PCE of 17.62% could be achieved [132]. Especially, some types of QDs with different functional groups and an efficient processing method exhibit outstanding long-term humidity

stability. Liu et al. [133] demonstrated chlorine-terminated Ti₃C₂ quantum dots (Ti₃C₂Cl_x QDs) as additives in perovskite precursor. The advantageous properties of the Cl-group in Ti₃C₂Cl_x QDs can form a strong bond with Pb²⁺ ions from the perovskite composition. In comparison to the hydroxyl (-OH) group in Ti₃C₂OH_x QDs, the perovskite solar cells could degrade significantly due to the Lewis acid-base reaction between -OH and organic amine groups in perovskite. This work showed that Ti₃C₂Cl_x QDs in devices without encapsulation maintained the PCEs greater than 84% for aging 1000 h under humidity testing in dark conditions [133].

3.3.2.4. Quantum dots in the hole-transporting layer (HTL). Several studies have shown that both organic and metallic QDs are also applicable for the HTL layer of perovskite solar cells: For example, so-called carbon QDs, which have a quantum-sized graphite structure and are an eco-friendly alternative to metal-based QDs [134], can be used as HTL materials to fabricate perovskite devices with documented efficiencies of 3% [85]. To minimize the defects in perovskite films, also graphene quantum dots (GQDs) were introduced into the perovskite films. This resulted in a smooth surface without pinholes, excellent conductivity, and light absorption, superior charge extraction, and a smaller leakage of current [135]. Regarding heavy metal-based QDs, Hu et al. reported a PCE of 7.5% for planar heterojunction perovskite solar cells using PbS colloidal quantum dots (average size 3 nm) as hole-transporters [136]. Rao et al. found a PCE of inverting planar heterojunction perovskite solar cells over 16% using CuS nanoparticles modified on the surface of indium tin oxide as hole-selective contacts [137]. CuInS₂ QDs as inorganic hole

Table 4. Summary of QDs and their optoelectric properties which were used in perovskite solar cells as active absorber, HTL, or ETL materials.

Type of QDs	Size (nm)	Cell architecture	Area (cm ²)	J _{sc} (mA/cm ²)	V _{oc} (V)	FF	PEC (%)	Ref.
QDs in Active Layer								
CsPbI ₃	-	FTO/TiO ₂ /CsPbI ₃ /spiro-OMeTAD/MoO _x /Al	0.10	13.47	1.23	0.65	10.77	[128]
MAPbBr _{0.9} I _{2.1}	-	FTO/TiO ₂ /MAPbI ₃ /MAPbBr _{0.9} I _{2.1} QDs/spiro-OMeTAD/Au	-	19.51	0.95	0.72	13.32	[129]
MAPbI ₃ : SnS	-	FTO/TiO ₂ /MAPI (with SnS QDs)/spiro-OMeTAD/Au	-	22.70	1.04	0.72	16.80	[130]
CsPbCl ₃ : Mn	~8	FTO/TiO ₂ /CsPbI ₃ : Mn QDs/spiro-OMeTAD/Au	-	22.03	1.11	0.76	18.57	[93]
MAPbI ₃ : Graphene	~3	FTO/TiO ₂ /MAPbI ₃ (with graphene QDs)/spiro-OMeTAD/Au	-	23.86	1.13	0.70	18.90	[135]
MAPbI ₃ : PbS	4	FTO/TiO ₂ /MAPbI ₃ (with PbS QDs)/spiro-OMeTAD/Au	-	23.50	1.03	0.77	18.60	[131]
MAPbI ₃ : Graphene	-	FTO/TiO ₂ /MAPbI ₃ -GQDs/spiro-OMeTAD/Au	0.09	22.49	1.03	0.76	17.62	[132]
QDs in HTL								
Black phosphorus	5.2	ITO/PEDOT: PSS-BPQDs/MAPbI ₃ /PCBM/Ag	-	20.56	1.01	0.80	16.69	[139]
Black phosphorus	3–10	ITO/BP QDs/FA _{0.85} MA _{0.15} PbBr _{0.5} I _{2.5} /spiro-OMeTAD/Au	0.09	16.77	1.03	0.65	11.26	[140]
Carbon	-	FTO/TiO ₂ /mp-TiO ₂ /MAPbI ₃ /Carbon QDs/Au	-	7.83	0.52	0.74	3.00	[86]
CuInS ₂	-	FTO/TiO ₂ /CH ₃ NH ₃ PbI ₃ /CuInS ₂ /ZnS/Au	-	18.60	0.92	0.49	8.38	[138]
PbS	-	FTO/TiO ₂ /MAPbI ₃ -PbS QDs/Au	0.12	24.63	0.34	0.43	3.60	[141]
PbS	-	ITO/ZnO/MAPbI ₃ -PbS/PbS/Au	-	21.80	0.61	0.68	8.95	[142]
PbS colloidal	-	ITO/PbS CQDs/CH ₃ NH ₃ PbI ₃ /PCBM/Al	-	12.10	0.86	0.72	7.50	[136]
CuS	-	ITO/CuS/CH ₃ NH ₃ PbI ₃ /C60/BCP/Ag	0.10	22.30	1.02	0.71	16.00	[137]
CuInS ₂	-	ITO/CuInS ₂ /Al ₂ O ₃ /CH ₃ NH ₃ PbI ₃ : CdS/PC ₆₀ BM/Ag	0.04	23.80	0.95	0.73	16.50	[156]
CdSe	2–4	FTO/TiO ₂ /CH ₃ NH ₃ PbI ₃ /CdSe/spiro-OMeTAD/Au	-	20.40	-	-	17.00	[155]
Cu ₂ ZnSnS ₄	~10	FTO/TiO ₂ /CH ₃ NH ₃ PbI ₃ /Cu ₂ ZnSnS ₄ /Au	0.15	18.75	0.95	0.61	10.72	[157]
Cu ₂ ZnSnSe ₄	~10	FTO/TiO ₂ /CH ₃ NH ₃ PbI ₃ /Cu ₂ ZnSnSe ₄ /Au	0.15	19.37	0.81	0.62	9.72	[157]
PbS	3.6	FTO/TiO ₂ /CH ₃ NH ₃ PbI ₃ /PbS/spiro-OMeTAD/Au	0.09	18.69	0.87	0.49	7.88	[143]
QDs in ETL								
PbS	~5	FTO/TiO ₂ /PbS/MAPbI ₃ /P3HT/Pt	0.10	6.30	0.88	0.49	4.92	[88]
CdS	-	FTO/TiO ₂ -CdS/MAPbI ₃ /spiro-OMeTAD/Au	0.10	18.00	0.91	0.67	9.90	[89]
Carbon	~10	ITO/TiO ₂ (with Carbon QDs)/MAPbI _{3-x} Cl _x /spiro-OMeTAD/Au	-	21.36	1.14	0.78	18.90	[158]
CdS	-	FTO/TiO ₂ /CdS/MAPbI ₃ /spiro-OMeTAD/Au	-	17.54	0.98	0.71	12.20	[147]
Graphene	~5	ITO/PCBM (with GQDs)/MAPbI ₃ /spiro-OMeTAD/Au	0.40	22.03	1.09	0.73	17.56	[153]
Graphene	5	FTO/ZnO (with GQDs)/CH ₃ NH ₃ PbI ₃ /spiro-OMeTAD/Au	0.15	21.70	1.03	0.68	15.20	[90]
CdSe	~10	ITO/PEDOT: PSS/CH ₃ NH ₃ PbI _{3-x} Cl _x /PCBM (with CdSe)/Rhodamine101/LiF/Ag	0.11	20.96	0.90	0.73	13.73	[92]
Carbon dots	~4.8	FTO/TiO ₂ (with Carbon dots)/MAPbCl _{1.3-x} I _{3-x} /spiro-OMeTAD/Au	-	22.64	1.02	0.72	16.40	[91]
Carbon dots	-	FTO/TiO ₂ /Carbon QDs/MAPbI ₃ /Carbon	0.14	16.40	0.79	0.61	7.62	[154]
Graphene	~4	FTO/ZnO-Graphene/CH ₃ NH ₃ PbI ₃ /spiro-OMeTAD/Au	-	22.80	1.05	0.72	17.20	[90]
CdS nanorods	-	ITO/CdS NRs array/perovskite/spiro-OMeTAD/MoO ₃ /Ag	0.05	18.77	0.93	0.50	8.36	[146]
Graphene	-	FTO/TiO ₂ /GQDs/CH ₃ NH ₃ PbI ₃ /spiro-OMeTAD/Au	0.13	17.06	0.94	0.64	10.15	[159]
Zn ₂ SnO ₄	~5.7	ITO/Zn ₂ SnO ₄ /MAPb(I _{0.9} Br _{0.1}) ₃ /PTAA*	-	20.40	1.11	0.73	16.50	[149]
ZnO	-	ITO-PET/Graphene/ZnO-QDs/CH ₃ NH ₃ PbI ₃ /spiro-OMeTAD/Ag	-	16.80	0.94	0.62	9.73	[148]
TiO ₂	3.6	FTO/TiO ₂ QDs/CH ₃ NH ₃ PbI ₃ /spiro-OMeTAD/Au	0.13	22.48	1.06	0.71	16.97	[160]
Graphene	7–14	FTO/TiO ₂ (with GQDs)/CH ₃ NH ₃ PbI ₃ /spiro-OMeTAD/Au	0.11	22.47	1.12	0.62	9.73	[161]
Graphene: SnO ₂	5–10	ITO/SnO ₂ (with GQDs)/CH ₃ NH ₃ PbI ₃ /spiro-OMeTAD/Au	0.10	23.05	1.13	0.78	20.31	[87]
γ-graphdiyne (GD)	3–5	FTO/TiO ₂ (with GD QDs)/CH ₃ NH ₃ PbI ₃ /spiro-OMeTAD/Au	0.09	22.48	1.12	0.79	19.89	[162]

*Spiro-OMeTAD: 2,2',7,7'-tetrakis (N,N-di-pmethoxyphenyl)- mine)–9,9'-spirobifluorene, BCP: Bathocuproine, PTAA: Poly[bis(4-phenyl) (2,4,6-trimethylphenyl)amine], PET: Polyethylene terephthalate.

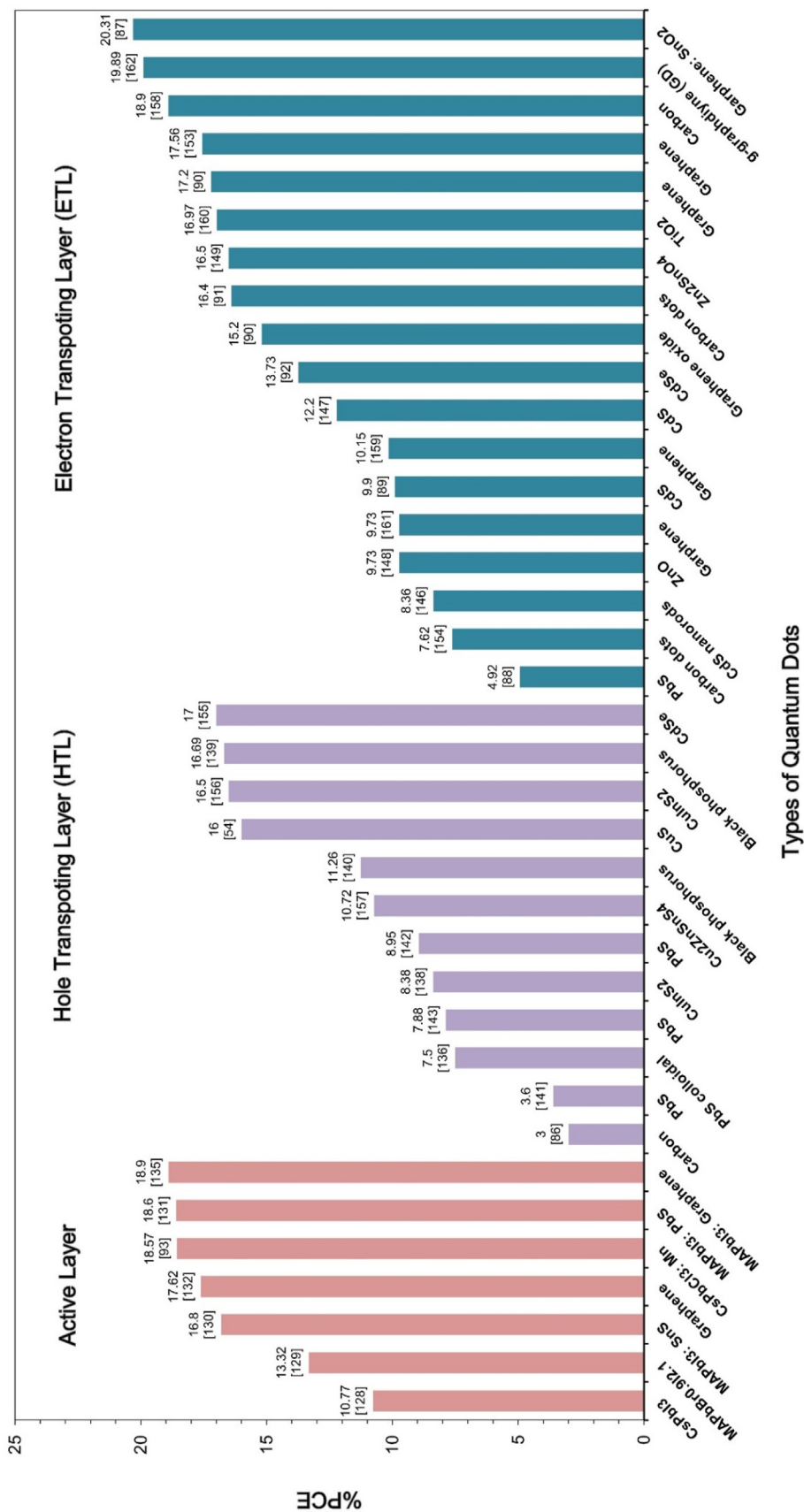


Figure 6. Comparison of different power conversion efficiencies with each of QDs for the active layer, HTL, and ETL.

conductors for perovskite solar cells were investigated by Lv et al. Cation exchange modification of the surface of CuInS_2 QDs to form $\text{CuInS}_2/\text{ZnS}$ core/shell heterostructure QDs resulted in a PCE of 8.38% [138].

In the following section, we discuss organic materials composed of QDs, such as QD-convened organic polymers. Chen et al. used black phosphorus QDs (BPQDs) deposited on poly(3,4-ethylenedioxythiophene) polystyrene sulfonate (PEDOT:PSS) films on the anode side of pin planar hybrid perovskite solar cells with the following structure: ITO/PEDOT: PSS:BPQDs/MAPbI₃/PCBM/Ag. This experiment demonstrated that BPQDs deposited on polymer films significantly improve hole extraction and photon conversion efficiency in comparison to the reference system [139]. For complete flexible perovskite devices, BPQDs (diameter ranged from 3 to 10 nm) with a PCE of 11.26% were constructed as ETL on ITO/PEN (indium tin oxide coated on polyethylene-naphthalate) substrates [140]. Meanwhile, BPQDs had the ability to decrease the trap state in the perovskite film, resulting in improved crystallization and recombination losses. Apart from that, incorporating QDs into light-harvesting materials is one of the strategies for improving photovoltaic efficiency. Some studies reported that the fabrication of perovskite solar systems using PbS-QDs as HTL (both one-step and two-step methods were used) resulted in a decrease in charge recombination and a longer absorption peak in the visible and near-infrared (NIR) range [136, 141, 142, 143].

3.3.2.5. Quantum dots in electron transport layer (ETL). Using QDs as ETL is one technique to increase PSC performance. These solar cells require low-temperature solutions. Unlike perovskite layers, ETL is made of TiO_2 calcined at high temperatures. It is used in perovskite solar cells because it has high performance and low hysteresis but has metal-oxide preparation restrictions [144, 145]. Moreover, the photocatalytic activity of TiO_2 also limits visible light absorption and fast electron-hole recombination.

Many reports introduced QDs to the ETL layer, where an inorganic semiconductor was replaced with planar structures through a solution process using CdS [108]. The fabrication of planar photovoltaic devices based on CdS was successfully performed, with the best cell exceeding 15% in PCE [144] and 11.2% PCE under reverse scan conditions [145]. Gu et al. demonstrated the hydrothermally synthesized planar heterostructure hybrid perovskite solar cells used CdS nanorods (CdS NRs) arrays as an electron transporter. The devices configured as an ITO/CdS NRs array/perovskite/spiro-OMeTAD/MoO₃/Ag array achieved the highest efficiency of 8.36% with an active area of 0.05 cm² after a 10-minute UV ozone treatment [146]. Hwang and Yong demonstrated that using CdS as a hole-blocking layer instead of the more conventional compact TiO_2 layer improved the photostability of perovskite solar cells. As a result, it was demonstrated that perovskite solar cells with the CdS layer exhibit significantly improved photostability, retaining over 90% of their initial efficiency after 12 h of sunlight illumination, while the TiO_2 perovskite solar cell retained only 18% of its initial efficiency under the same conditions [147]. Ameen et al. fabricated flexible perovskite devices with a 9.73% PCE using ZnO QDs deposited on flexible ITO-PET/graphene thin films through a spin coating approach [148]. With methylammonium lead halide [MAPb(I_{0.9}Br_{0.1})₃], zinc stannate (Zn₂SnO₄) particles with a size of 10 nm could achieve a PCE of 16.0% [149].

QD-sensitized solar cells are typically well-characterized QD-materials incorporated into a nanostructure semiconductor (e.g., TiO_2 , ZnO) by one of three processes: electrodeposition, chemical bath deposition, or successive ionic layer adsorption and reaction (SILAR) [150]. Due to the fact that the hole-electron pairs were formed under illuminated conditions; their charge carriers combine at the semiconductor-QD interface. Recombination of charge carriers results in photocurrent failure, but also in the instability of the liquid electrolyte, lowering the efficiency of the solar cell. The primary advantage of QDs as sensitizers in the cell,

however, is their tunable but size-dependent bandgap properties [98, 108, 109, 151]. Thus, in perovskite devices, QDs are deposited on the surface of the semiconductors or incorporated into a mesoporous TiO_2 . PbS QDs (with a diameter of 5 nm) are deposited on crystalline TiO_2 photoanode films using the SILAR process as part of the QD-composed inorganic materials. The PbS QDs were observed to act as a NIR light absorber and a surface-blocking layer [88]. Following that, the addition of a CdS/ TiO_2 electrode with a core/shell structure could improve the stability under illumination of perovskite solar cells. Additionally, the TiO_2 /CdS core/shell structure was used as an electron transporter in perovskite photovoltaic cells to passivate surface trap sites on the TiO_2 layer [89].

The incorporation of carbon QDs (average diameter 4.8 nm) into a mesoporous TiO_2 layer can improve the electron transfer capability. PCE of 16.4% is possible [91, 112]. The synthesis of graphene quantum dots (with a variable size of 3–10 nm) was carried out using ZnO and TiO_2 layers [90, 152]. By using quick electron extraction, graphene quantum dots (GQDs) can be induced and improve the PCE up to 10%. Regarding organic materials composed of QDs as ETL, an optimized content of 5% CdSe/PCBM composite resulted in an acceptable PCE of 13.7% for inverted planar perovskite devices [92]. Yang also registered different graphene quantum dot concentrations in PCBM solutions using the fabricated structure ITO/PCBM/MAPbI₃/spiro-OMeTAD/Au. A PCE of 17.5% was observed when 0.5%wt GQDs (with a size of 5 nm) were combined with PCBM solution [153]. Carbon QDs with different uniform diameters of 3–5 nm were introduced into perovskite films, and their effects on the performance of TiO_2 nanosheet-based perovskite films resulted in a PCE of 7.62% [154].

To demonstrate the further value of QDs, Figure 6 compares the efficiency of perovskite solar cells with and without various forms of QDs as an active absorber (pink-bar section), an HTL (purple-bar section), and an ETL (blue-bar section). To improve the efficiency of perovskite devices, several different quantum dots were used. This graph depicts the low to high power conversion efficiencies in three parts, from left to right. It was observed that the function of QDs in the development of perovskite solar cells earned maximum efficiencies of 17.0% [155] 18.9% [92], and 20.3% [87] for CsPbCl₃: Mn (a photoactive absorber), CdSe (a hole collecting layer), and graphene: SnO₂ (an electron transporting layer), respectively, even though, the real active area of high-performance solar cells is still small (0.10 cm²).

4. Conclusions and outlook

The sensitivity of perovskite solar cells towards environmental factors is a major consideration and has to be addressed for becoming a commercial industrial technology. This review discusses the stabilization of perovskite solar cells, particularly against humid environments by using internal additive materials that passivate the surface by small linker molecules, polymers, or photo-stabilizing agents, such as quantum dots. This article discusses a variety of QD types used in conventional and inverted perovskite solar cells. QDs in perovskite solar cells allowed the improvement of the performance with recent power conversion efficiencies approaching 20%. QDs that were implemented in perovskite sheets, HTL, and ETL demonstrated an improvement in the efficiency of perovskite solar cells, which is summarized in this review. The implementation of QDs in perovskite cells resulted in the reduction of the recombination pathways, which in turn resulted in the long-term stability of perovskite devices.

Challenges, such as stability issues, necessitate additional research into processing routes toward improved product quality in order to advance perovskite technology. The back electrode (i.e., Au, and Ag) is mostly used for perovskite designs, but it is not suitable for pushing the perovskite photovoltaic market. Ag, which is the cheaper material, reacts with the halides, e.g., iodide from perovskite, and forms AgI, which

results in a loss of the device performance, while Au electrode is mostly inert but far more expensive. In addition, transparent conducting oxide electrodes are necessary to replace metal-based materials, which would allow the evolution of perovskite-based tandem solar cells. On the other hand, carbon materials as a top electrode are also applied for flexible perovskite solar cells due to excellent electric and optical, low cost, upscale fabrication technique, as well as improved perovskite lifetime. However, the International Summit on Organic Photovoltaic Stability (ISOS) protocols (i.e., dark storage (ISOS-D), light soaking (ISOS-L), etc.) [163] are required to examine the perovskite operational stability and real testing outdoor stability (ISOS-O) [163] to determine effects of weather on the perovskite modules, which is necessary for commercial application in near future.

An advantage of perovskite photovoltaic to succeed in the energy market is the manufacturing cost, which corresponds to the leveled cost of electricity (LCOE) of about 3.5–4.9 US cents/kWh, which is cheaper than traditional energy sources [164]. However, cost analysis of perovskite-silicon and perovskite-perovskite tandem modules were evaluated to be 5.22 and 4.22 US cents/kWh, respectively [165], which may become cheaper with the advances in electrode materials. Therefore, the future status of the perovskite photovoltaic field might be unveiled for the next-generation photovoltaic field.

Declarations

Author contribution statement

All authors listed have significantly contributed to the development and the writing of this article.

Funding statement

Surawut Chuangchote and Kanyanee Sanglee were supported by Energy Innovation Program, Technology Development Groups (TDGs) project of National Science and Technology Development Agency (NSTDA), Thailand (grant no P2051358). Eva-Kathrin Ehmoser and FlorianPart were supported by The Federal Ministry for Climate Action, Environment, Energy, Mobility, Innovation and Technology who supported the NANO Environmental Health and Safety research project “SolarCircle” (project no. 880277).

Data availability statement

Data included in article/supplementary material/referenced in article.

Declaration of interests statement

The authors declare no conflict of interest.

Additional information

No additional information is available for this paper.

References

- [1] R. Deng, N.L. Chang, Z. Ouyang, C.M. Chong, A techno-economic review of silicon photovoltaic module recycling, *Renew. Sustain. Energy Rev.* 109 (2019) 532–550.
- [2] M. Tao, V. Fthenakis, B. Ebin, B.M. Steenari, E. Butler, P. Sinha, E.S. Simon, Major challenges and opportunities in silicon solar module recycling, *Prog. Photovoltaics Res. Appl.* 28 (2020) 1077–1088.
- [3] P.K. Nayak, S. Mahesh, H.J. Snaith, D. Cahen, Photovoltaic solar cell technologies: analysing the state of the art, *Nat. Rev. Mater.* 4 (2019) 269–285.
- [4] A. Kojima, K. Teshima, Y. Shirai, T. Miyasaka, Organometal halide perovskites as visible-light sensitizers for photovoltaic cells, *J. Am. Chem. Soc.* 131 (2009) 6050–6051.
- [5] W.S. Yang, J.H. Noh, N.J. Jeon, Y.C. Kim, S. Ryu, J. Seo, S.I. Seok, High-performance photovoltaic perovskite layers fabricated through intramolecular exchange, *Science* 348 (2015) 1234–1237.
- [6] G. Yang, H. Tao, P. Qin, W. Ke, G. Fang, Recent progress in electron transport layers for efficient perovskite solar cells, *J. Mater. Chem. A* 4 (2016) 3970–3990.
- [7] J. Zhang, W. Zhang, H.M. Cheng, S.R.P. Silva, Critical review of recent progress of flexible perovskite solar cells, *Mater. Today* 39 (2020) 66–88.
- [8] D. Angmo, G. DeLuca, A.D. Scully, A.S. Chesman, A. Seeber, C. Zuo, M. Gao, A lab-to-fab study toward roll-to-roll fabrication of reproducible perovskite solar cells under ambient room conditions, *Cell Rep.* 2 (2021), 100293.
- [9] NREL, The National Renewable Energy Laboratory Chart, 2021 accessed.
- [10] W. Chen, Y. Wu, Y. Yue, J. Liu, W. Zhang, X. Yang, L. Han, Efficient and stable large-area perovskite solar cells with inorganic charge extraction layers, *Science* 350 (6263) (2015).
- [11] M.M. Lee, J. Teuscher, T. Miyasaka, T.N. Murakami, H.J. Snaith, Efficient hybrid solar cells based on meso-superstructured organometal halide perovskites, *Science* 338 (2012) 643–647.
- [12] S. Chen, X. Dai, S. Xu, H. Jiao, L. Zhao, J. Huang, Stabilizing perovskite-substrate interfaces for high-performance perovskite modules, *Science* 373 (6557) (2021) 902–907.
- [13] H. Zhou, Q. Chen, G. Li, S. Luo, T.B. Song, H.S. Duan, Y. Yang, Interface engineering of highly efficient perovskite solar cells, *Science* 345 (2014) 542–546.
- [14] M.A. Green, A. Ho-Baillie, H.J. Snaith, The emergence of perovskite solar cells, *Nat. Photonics* 8 (2014) 506–514.
- [15] A. Phaometvarithorn, S. Chuangchote, P. Kumnorkaew, J. Wootthikanokkhan, Hybrid solar cells composed of perovskite and polymer photovoltaic structures, *Solid State Electron.* 144 (2018) 7–12.
- [16] S. Brittan, G.W.P. Adhyaksa, E.C. Garnett, The expanding world of hybrid perovskites: materials properties and emerging applications, *MRS Commun* 5 (2015) 7–26.
- [17] M. Petrović, V. Chellappan, S. Ramakrishna, Perovskites: solar cells & engineering applications—materials and device developments, *Sol. Energy* 122 (2015) 678–699.
- [18] W.J. Yin, T. Shi, Y. Yan, Unusual defect physics in $\text{CH}_3\text{NH}_3\text{PbI}_3$ perovskite solar cell absorber, *Appl. Phys. Lett.* 104 (2014), 063903.
- [19] C.R. Kagan, C.B. Murray, Charge transport in strongly coupled quantum dot solids, *Nat. Nanotechnol.* 10 (2015) 1013–1026.
- [20] S. Bonabi Naghadeh, B. Luo, G. Abdelmageed, Y.C. Pu, C. Zhang, J.Z. Zhang, Photophysical properties and improved stability of organic–inorganic perovskite by surface passivation, *J. Phys. Chem. C* 122 (2018) 15799–15818.
- [21] J. Yang, B.D. Siempelkamp, D. Liu, T.L. Kelly, Investigation of $\text{CH}_3\text{NH}_3\text{PbI}_3$ degradation rates and mechanisms in controlled humidity environments using in situ techniques, *ACS Nano* 9 (2015) 1955–1963.
- [22] J. Zhao, B. Cai, Z. Luo, Y. Dong, Y. Zhang, H. Xu, C. Gao, Investigation of the hydrolysis of perovskite organometallic halide $\text{CH}_3\text{NH}_3\text{PbI}_3$ in humidity environment, *Sci. Rep.* 6 (2016), 21976.
- [23] A. Abate, Perovskite solar cells go lead free, *Joule* 1 (2017) 659–664.
- [24] S. Svanström, A.G. Fernández, T. Sloboda, T.J. Jacobsson, H. Rensmo, U.B. Cappel, X-Ray stability and degradation mechanism of lead halide perovskites and lead halides, *Phys. Chem. Chem. Phys.* 23 (2021) 12479–12489.
- [25] B. Philippe, B.W. Park, R. Lindblad, J. Oscarsson, S. Ahmadi, E.M. Johansson, H. Rensmo, Chemical and electronic structure characterization of lead halide perovskites and stability behavior under different exposures: a photoelectron spectroscopy investigation, *Chem. Mater.* 27 (2015) 1720–1731.
- [26] J.M. Frost, K.T. Butler, F. Brivio, C.H. Hendon, M. Van Schilfgaarde, A. Walsh, Atomistic origins of high-performance in hybrid halide perovskite solar cells, *Nano Lett.* 14 (2014) 2584–2590.
- [27] J.A. Christians, P.A. Miranda Herrera, P.V. Kamat, Transformation of the excited state and photovoltaic efficiency of $\text{CH}_3\text{NH}_3\text{PbI}_3$ perovskite upon controlled exposure to humidified air, *J. Am. Chem. Soc.* 137 (2015) 1530–1538.
- [28] F. El-Mellouhi, A. Marzouk, E.T. Bentría, S.N. Rashkeev, S. Kais, F.H. Alharbi, Hydrogen bonding and stability of hybrid organic–inorganic perovskites, *Chem. Sus. Chem* 9 (2016) 2648–2655.
- [29] S. Singh, D. Kabra, Defects in halide perovskite semiconductors: impact on photo-physics and solar cell performance, *J. Phys. D Appl. Phys.* 53 (2020), 503003.
- [30] M. Nukunodompanich, G. Budiutama, K. Suzuki, K. Hasegawa, M. Ihara, Dominant effect of the grain size of the MAPbI_3 perovskite controlled by the surface roughness of TiO_2 on the performance of perovskite solar cells, *Cryst. Eng. Comm.* 22 (2020) 2718–2727.
- [31] T. Leijtens, G.E. Eperon, S. Pathak, A. Abate, M.M. Lee, H.J. Snaith, Overcoming ultraviolet light instability of sensitized TiO_2 with meso-superstructured organometal tri-halide perovskite solar cells, *Nat. Commun.* 4 (2013) 1–8.
- [32] B. McKenna, J.R. Troughton, T.M. Watson, R.C. Evans, Enhancing the stability of organolead halide perovskite films through polymer encapsulation, *RSC Adv.* 7 (2017) 32942–32951.
- [33] Y. Hu, T. Niu, Y. Liu, Y. Zhou, Y. Xia, C. Ran, W. Huang, Flexible perovskite solar cells with high power-per-weight: progress, application, and perspectives, *ACS Energy Lett.* 6 (2021) 2917–2943.
- [34] Q. Wang, Q. Dong, T. Li, A. Gruverman, J. Huang, Thin insulating tunneling contacts for efficient and water-resistant perovskite solar cells, *Adv. Mater.* 28 (2016) 6734–6739.
- [35] C.C. Boyd, R. Cheacharoen, T. Leijtens, M.D. McGehee, Understanding degradation mechanisms and improving stability of perovskite photovoltaics, *Chem. Rev.* 119 (2019) 3418–3451.
- [36] J. Kim, A. Ho-Baillie, S. Huang, Review of novel passivation techniques for efficient and stable perovskite solar cells, *Sol. RRL* 3 (2019), 1800302.
- [37] J. Zhang, Z. Hu, L. Huang, G. Yue, J. Liu, X. Lu, Y. Zhu, Bifunctional alkyl chain barriers for efficient perovskite solar cells, *Chem. Commun.* 51 (2015) 7047–7050.

- [38] H. Xiong, Y. Rui, Y. Li, Q. Zhang, H. Wang, Hydrophobic coating over a $\text{CH}_3\text{NH}_3\text{PbI}_3$ absorbing layer towards air stable perovskite solar cells, *J. Mater. Chem. Chem. C* 4 (2016) 6848–6854.
- [39] H. Zhu, B. Huang, S. Wu, Z. Xiong, J. Li, W. Chen, Facile surface modification of $\text{CH}_3\text{NH}_3\text{PbI}_3$ films leading to simultaneously improved efficiency and stability of inverted perovskite solar cells, *J. Mater. Chem. A* 6 (2018) 6255–6264.
- [40] J. Cao, J. Yin, S. Yuan, Y. Zhao, J. Li, N. Zheng, Thiols as interfacial modifiers to enhance the performance and stability of perovskite solar cells, *Nanoscale* 7 (2015) 9443–9447.
- [41] G. Abdelmageed, H.R. Sully, S. Bonabi Naghadeh, A. El-Hag Ali, S.A. Carter, J.Z. Zhang, Improved stability of organometal halide perovskite films and solar cells toward humidity via surface passivation with oleic acid, *ACS Appl. Energy Mater.* 1 (2018) 387–392.
- [42] D. Koushik, W.J. Verhees, Y. Kuang, S. Veenstra, D. Zhang, M.A. Verheijen, R.E. Schropp, High-efficiency humidity-stable planar perovskite solar cells based on atomic layer architecture, *Energy Environ. Sci.* 10 (2017) 91–100.
- [43] G. Zhang, Y. Zheng, Y. Shi, X. Ma, M. Sun, T. Li, Y. Shao, Improving the performance of perovskite solar cells with insulating additive-modified hole transport layers, *ACS Appl. Mater. Interfaces* 14 (2022) 11500–11508.
- [44] X. Wang, K. Rakstys, K. Jack, H. Jin, J. Lai, H. Li, P.E. Shaw, Engineering fluorinated-cation containing inverted perovskite solar cells with an efficiency of > 21% and improved stability towards humidity, *Nat. Commun.* 12 (2021) 1–10.
- [45] K. Lee, H. Yu, J.W. Lee, J. Oh, S. Bae, S.K. Kim, J. Jang, Efficient and moisture-resistant hole transport layer for inverted perovskite solar cells using solution-processed polyaniline, *J. Mater. Chem. C* 6 (2018) 6250–6256.
- [46] T. Wang, Y. Li, Q. Cao, J. Yang, B. Yang, X. Pu, X. Li, Deep defect passivating and shallow vacancy repairing via ionic silicone polymer toward highly stable inverted perovskite solar cells, *Energy Environ. Sci.* 15 (2022) 4414–4424.
- [47] M. Loizos, M. Tountas, N. Tzoganakis, C.L. Chochos, A. Nega, A. Schiza, E. Kymakis, Enhancing the lifetime of inverted perovskite solar cells using a new hydrophobic hole transport material, *Energy Advances* 1 (2022) 312–320.
- [48] Y.R. Kim, J. Kim, H. Kim, C.J. Yoon, J.T. Yun, J.H. Kim, K. Lee, Inner encapsulating approach for moisture-stable perovskite solar cells, *Solar RRL* 5 (2021), 2100351.
- [49] D.J. Fairfield, H. Sai, A. Narayanan, J.V. Passarelli, M. Chen, J. Palasz, S.I. Stupp, Structure and chemical stability in perovskite–polymer hybrid photovoltaic materials, *J. Mater. Chem. A* 7 (2019) 1687–1699.
- [50] D. Bryant, N. Aristidou, S. Pont, I. Sanchez-Molina, T. Chotchanangatchaval, S. Wheeler, S.A. Haque, Light and oxygen induced degradation limits the operational stability of methylammonium lead triiodide perovskite solar cells, *Energy Environ. Sci.* 9 (2016) 1655–1660.
- [51] W. Xiang, Q. Chen, Y. Wang, M. Liu, F. Huang, T. Bu, X. Zhao, Improved air stability of perovskite hybrid solar cells via blending poly(dimethylsiloxane)–urea copolymers, *J. Mater. Chem. A* 5 (2017) 5486–5494.
- [52] D. Bi, C. Yi, J. Luo, J.D. Décoppet, F. Zhang, S.M. Zakeeruddin, M. Grätzel, Polymer-templated nucleation and crystal growth of perovskite films for solar cells with efficiency greater than 21%, *Nat. Energy* 1 (2016), 16142.
- [53] Y. Zhao, J. Wei, H. Li, Y. Yan, W. Zhou, D. Yu, Q. Zhao, A polymer scaffold for self-healing perovskite solar cells, *Nat. Commun.* 7 (2016), 10228.
- [54] C. Sun, Y. Guo, B. Fang, J. Yang, B. Qin, H. Duan, H. Liu, Enhanced photovoltaic performance of perovskite solar cells using polymer P(VDF-TrFE) as a processed additive, *J. Phys. Chem. C* 120 (2016) 12980–12988.
- [55] B. Li, Y. Zhang, L. Fu, T. Yu, S. Zhou, L. Zhang, L. Yin, Surface passivation engineering strategy to fully-inorganic cubic CsPbI_3 perovskites for high-performance solar cells, *Nat. Commun.* 9 (2018) 1–8.
- [56] R. Zheng, S. Zhao, H. Zhang, H. Li, J. Zhuang, X. Liu, H. Wang, Defect passivation grain boundaries using 3-aminopropyltrimethoxysilane for highly efficient and stable perovskite solar cells, *Sol. Energy* 224 (2021) 472–479.
- [57] S. Zhao, M. Qin, Y. Xiang, H. Wang, J. Xie, L. Gong, K. Yan, Bifunctional effects of trichloro (octyl) silane modification on the performance and stability of a perovskite solar cell via microscopic characterization techniques, *ACS Appl. Energy Mater.* 3 (2020) 3302–3309.
- [58] L. Xie, J. Chen, P. Vashishtha, X. Zhao, G.S. Shin, S.G. Mhaisalkar, N.G. Park, Importance of functional groups in cross-linking methoxysilane additives for high-efficiency and stable perovskite solar cells, *ACS Energy Lett.* 4 (2019) 2192–2200.
- [59] S. Narendhiran, A. Kunka Ravindran, I.D. Rajan Thomas, S.P. Muthu, R. Perumalsamy, Poly (vinylidene fluoride-co-hexafluoropropylene) additive in perovskite for stable performance of carbon-based perovskite solar cells, *Int. J. Energy Res.* 46 (2022) 1565–1574.
- [60] L. Li, S. Tu, G. You, J. Cao, D. Wu, L. Yao, Q. Ling, Enhancing performance and stability of perovskite solar cells through defect passivation with a polyamide derivative obtained from benzoxazine-isocyanide chemistry, *J. Chem. Eng.* 431 (2022), 133951.
- [61] J. Yang, Q. Cao, Z. He, X. Pu, T. Li, B. Gao, X. Li, The poly(styrene-co-acrylonitrile) polymer assisted preparation of high-performance inverted perovskite solar cells with efficiency exceeding 22, *Nano Energy* 82 (2021), 105731.
- [62] Y. Mei, M. Sun, H. Liu, X. Li, S. Wang, Polymer additive assisted crystallization of perovskite films for high-performance solar cells, *Org. Electron.* 96 (2021), 106258.
- [63] Q. Cao, Y. Li, H. Zhang, J. Yang, J. Han, T. Xu, M. Grätzel, Efficient and stable inverted perovskite solar cells with very high fill factors via incorporation of star-shaped polymer, *Sci. Adv.* 7 (2021) eabg0633.
- [64] Ge, Y.; Ye, F.; Xiao, M.; Wang, H.; Wang, C.; Liang, J.; Fang, G. Internal encapsulation for lead halide perovskite films for efficient and very stable solar cells. *Adv. Energy Mater.* 2022, 2200361.
- [65] X. Li, M.I. Dar, C. Yi, J. Luo, M. Tschumi, S.M. Zakeeruddin, M. Grätzel, Improved performance and stability of perovskite solar cells by crystal crosslinking with alkylphosphonic acid ω -ammonium chlorides, *Nat. Chem.* 7 (2015) 703–711.
- [66] B. Li, C. Fei, K. Zheng, X. Qu, T. Pullerits, G. Cao, J. Tian, Constructing water-resistant $\text{CH}_3\text{NH}_3\text{PbI}_3$ perovskite films via coordination interaction, *J. Mater. Chem. A* 4 (2016) 17018–17024.
- [67] C.R. Kagan, C.B. Murray, Charge transport in strongly coupled quantum dot solids, *Nat. Nanotechnol.* 10 (2015) 1013–1026.
- [68] S. Kumar, M. Nehra, A. Deep, D. Kedia, N. Dilbaghi, K.H. Kim, Quantum-sized nanomaterials for solar cell applications, *Renew. Sustain. Energy Rev.* 73 (2017) 821–839.
- [69] G.H. Carey, A.L. Abdelhady, Z. Ning, S.M. Thon, O.M. Bakr, E.H. Sargent, Colloidal quantum dot solar cells. Chemical reviews, *Chem. Rev.* 115 (2015) 12732–12763.
- [70] J. Duan, H. Zhang, Q. Tang, B. He, L. Yu, Recent advances in critical materials for quantum dot-sensitized solar cells, *A Review. J. Mater. Chem. A* 3 (2015) 17497–17510.
- [71] J. Tang, E.H. Sargent, Infrared colloidal quantum dots for photovoltaics: fundamentals and recent progress, *Adv. Math.* 23 (2011) 12–29.
- [72] K. Rurack, Fluorescence Quantum Yields: Methods of Determination and Standards, *Standardization And Quality Assurance In Fluorescence Measurements I*, Springer, Berlin, Heidelberg, 2008, pp. 101–105.
- [73] M. Grabolle, M. Spieles, V. Lesnyak, N. Gaponik, A. Eychmüller, U. Resch-Genger, Determination of the fluorescence quantum yield of quantum dots: suitable procedures and achievable uncertainties, *Anal. Chem.* 81 (2009) 6285–6294.
- [74] J. Yuan, A. Hazarika, Q. Zhao, X. Ling, T. Moot, W. Ma, J.M. Luther, Metal halide perovskites in quantum dot solar cells: progress and prospects, *Joule* 4 (2020) 1160–1185.
- [75] Q. Chen, J. Wu, X. Ou, B. Huang, J. Almutlaq, A.A. Zhumekenov, X. Liu, All-inorganic perovskite nanocrystal scintillators, *Nature* 561 (2018) 88–93.
- [76] M.K. Herndon, A. Gupta, V. Kaydanov, R.T. Collins, Evidence for grain-boundary-assisted diffusion of sulfur in polycrystalline CdS/CdTe heterojunctions, *Appl. Phys. Lett.* 75 (1999) 3503–3505.
- [77] Y. Wu, N. Ding, Y. Zhang, B. Liu, X. Zhuang, S. Liu, H. Song, Toward broad spectral response inverted perovskite solar cells: insulating quantum-cutting perovskite nanophosphors and multifunctional ternary organic bulk-heterojunction, *Adv. Energy Mater.* 12 (2022), 2200005.
- [78] X. Wang, Y. Ma, Q. Wu, Z. Wang, Y. Tao, Y. Zhao, Z. Kang, Ultra-bright and stable pure blue light emitting diode from O, N Co-doped carbon dots, *Laser Photon. Rev.* 15 (2021), 2000412.
- [79] H. Xiao, J. Fu, X. Wei, B. Wang, Q. Qian, J. Huang, Z. Zang, Photoelectric-extractive and ambient-stable $\text{CsPbBr}_3/\text{SnO}_2$ nanocrystals for high-performance photodetection, *Laser Photon. Rev.* (2022), 2200276.
- [80] Y. Dongdong, Z. Shuangyi, Z. Yubo, W. Huaxin, Z. Zhigang, Highly efficient emission and high-CRI warm white light-emitting diodes from ligand-modified CsPbBr_3 quantum dots, *Opto-Electron. Adv.* 5 (2022), 200075.
- [81] L. Wang, L. Wang, C.J. Chen, K.C. Chen, Z. Hao, Y. Luo, H. Li, Green InGaN quantum dots breaking through efficiency and bandwidth bottlenecks of micro-LEDs, *Laser Photon. Rev.* 15 (2021), 2000406.
- [82] D. Yan, Q. Mo, S. Zhao, W. Cai, Z. Zang, Room temperature synthesis of Sn^{2+} doped highly luminescent CsPbBr_3 quantum dots for high CRI white light-emitting diodes, *Nanoscale* 13 (21) (2021) 9740–9746.
- [83] S.A. Veldhuis, P.P. Boix, N. Yantara, M. Li, T.C. Sum, N. Mathews, S.G. Mhaisalkar, Perovskite materials for light-emitting diodes and lasers, *Adv. Mater.* 28 (2016) 6804–6834.
- [84] X. Lan, O. Voznyy, F.P. García de Arquer, M. Liu, J. Xu, A.H. Proppe, E.H. Sargent, 10.6% certified colloidal quantum dot solar cells via solvent-polarity-engineered halide passivation, *Nano Lett.* 16 (2016) 4630–4634.
- [85] J.Z. Fan, N.T. Andersen, M. Biondi, P. Todorović, B. Sun, O. Ouellette, E.H. Sargent, Mixed lead halide passivation of quantum dots, *Adv. Mater.* 31 (2019), 1904304.
- [86] S. Paulo, G. Stoica, W. Cambarau, E. Martinez-Ferrero, E. Palomares, Carbon quantum dots as new hole transport material for perovskite solar cells, *Synth. Met.* 222 (2016) 17–22.
- [87] J. Xie, K. Huang, X. Yu, Z. Yang, K. Xiao, Y. Qiang, D. Yang, Enhanced electronic properties of SnO_2 via electron transfer from graphene quantum dots for efficient perovskite solar cells, *ACS Nano* 11 (2017) 9176–9182.
- [88] Y. Yang, W. Wang, Effects of incorporating PbS quantum dots in perovskite solar cells based on $\text{CH}_3\text{NH}_3\text{PbI}_3$, *J. Power Sources* 293 (2015) 577–584.
- [89] I. Hwang, M. Baek, K. Yong, Core/shell structured TiO_2/CdS electrode to enhance the light stability of perovskite solar cells, *ACS Appl. Mater. Interfaces* 7 (2015) 27863–27870.
- [90] M.M. Tavakoli, R. Tavakoli, S. Hasanzadeh, M.H. Mirfasihi, Interface engineering of perovskite solar cell using a reduced-graphene scaffold, *J. Phys. Chem. C* 120 (2016) 19531–19536.
- [91] J. Jin, C. Chen, H. Li, Y. Cheng, L. Xu, B. Dong, Q. Dai, Enhanced performance and photostability of perovskite solar cells by introduction of fluorescent carbon dots, *ACS Appl. Mater. Interfaces* 9 (2017) 14518–14524.
- [92] X. Zeng, T. Zhou, C. Leng, Z. Zang, M. Wang, W. Hu, M. Zhou, Performance improvement of perovskite solar cells by employing a CdSe quantum dot/PCBM composite as an electron transport layer, *J. Mater. Chem.* 5 (2017) 17499–17505.
- [93] Q. Wang, X. Zhang, Z. Jin, J. Zhang, Z. Gao, Y. Li, S.F. Liu, Energy-down-shift CsPbCl_3 : Mn quantum dots for boosting the efficiency and stability of perovskite solar cells, *ACS Energy Lett.* 2 (2017) 1479–1486.
- [94] X. Zheng, J. Troughton, N. Gasparini, Y. Lin, M. Wei, Y. Hou, O.M. Bakr, Quantum dots supply bulk-and surface-passivation agents for efficient and stable perovskite solar cells, *Joule* 3 (2019) 1963–1976.

- [95] X.Y. Yu, B.X. Lei, D.B. Kuang, C.Y. Su, Highly efficient CdTe/CdS quantum dot sensitized solar cells fabricated by a one-step linker assisted chemical bath deposition, *Chem. Sci.* 2 (2011) 1396–1400.
- [96] J. Bai, B. Zhou, Titanium dioxide nanomaterials for sensor applications, *Chem. Rev.* 114 (2014) 10131–10176.
- [97] J. Xu, Z. Chen, J.A. Zapien, C.S. Lee, W. Zhang, Surface engineering of ZnO nanostructures for semiconductor-sensitized solar cells, *Adv. Mater.* 26 (2014) 5337–5367.
- [98] P.V. Kamat, Quantum dot solar cells. The next big thing in photovoltaics, *J. Phys. Chem. Lett.* 4 (2013) 908–918.
- [99] Z. Du, M. Artemyev, J. Wang, J. Tang, Performance improvement strategies for quantum dot-sensitized solar cells, *A Review. J. Mater. Chem. A.* 7 (2019) 2464–2489.
- [100] W. Li, X. Zhong, Capping ligand-induced self-assembly for quantum dot sensitized solar cells, *J. Phys. Chem. Lett.* 6 (2015) 796–806.
- [101] S. Kumar, T. Nann, Shape control of II–VI semiconductor nanomaterials, *Small* 2 (2006) 316–329.
- [102] N.T. Thanh, N. Maclean, S. Mahiddine, Mechanisms of nucleation and growth of nanoparticles in solution, *Chem. Rev.* 114 (2014) 7610–7630.
- [103] C. Giansante, L. Carbone, C. Giannini, D. Altamura, Z. Ameer, G. Maruccio, G. Gigli, Colloidal arenethiolate-capped PbS quantum dots: optoelectronic properties, self-assembly, and application in solution-cast photovoltaics, *J. Phys. Chem. C* 117 (2013) 13305–13317.
- [104] I. Lokteva, N. Radychev, F. Witt, H. Borchert, J. Parisi, J. Kolny-Olesiak, Surface treatment of CdSe nanoparticles for application in hybrid solar cells: the effect of multiple ligand exchange with pyridine, *J. Phys. Chem. C* 114 (2010) 12784–12791.
- [105] J. Albero, P. Riente, J.N. Clifford, M.A. Pericàs, E. Palomares, Improving CdSe quantum dot/polymer solar cell efficiency through the covalent functionalization of quantum dots: implications in the device recombination kinetics, *J. Phys. Chem. C* 117 (2013) 13374–13381.
- [106] L. Wang, W. Fu, Z. Gu, C. Fan, X. Yang, H. Li, H. Chen, Low temperature solution processed planar heterojunction perovskite solar cells with a CdSe nanocrystal as an electron transport/extraction layer, *J. Mater. Chem. C* 2 (2014) 9087–9090.
- [107] H. Choi, P.K. Santra, P.V. Kamat, Synchronized energy and electron transfer processes in covalently linked CdSe-squaraine dye-TiO₂ light harvesting assembly, *ACS Nano* 6 (2012) 5718–5726.
- [108] K. Sanglee, S. Chuangchote, T. Krajangsang, J. Sritharithikhun, K. Sriprapha, T. Sagawa, Quantum dot-modified titanium dioxide nanoparticles as an energy-band tunable electron-transporting layer for open air-fabricated planar perovskite solar cells, *Nanomater. Nanotechnol.* 10 (2020), 1847980420961638.
- [109] F. Part, C. Zaba, O. Bixner, T.A. Grünwald, H. Michor, S. Küpcü, E.K. Ehmoser, Doping method determines para-or superparamagnetic properties of photostable and surface-modifiable quantum dots for multimodal bioimaging, *Chem. Mater.* 3 (2018) 4233–4241.
- [110] F. Li, S. Huang, X. Liu, Z. Bai, Z. Wang, H. Xie, H. Zhong, Highly stable and spectrally tunable gamma phase RbxCs_{1-x}PbI₃ gradient-alloyed quantum dots in PMMA matrix through A sites engineering, *Adv. Funct. Mater.* 31 (2021), 2008211.
- [111] M. Ruzyccka-Ayoush, P. Kowalik, A. Kowalczyk, P. Bujak, A.M. Nowicka, M. Wojewodzka, I.P. Grudzinski, Quantum dots as targeted doxorubicin drug delivery nanosystems, *Cancer Nano* 12 (2021) 1–27.
- [112] E. Zillner, S. Fengler, P. Niyamakom, F. Rauscher, K. Kohler, T. Dittrich, Role of ligand exchange at CdSe quantum dot layers for charge separation, *J. Phys. Chem. C* 116 (2012) 16747–16754.
- [113] R.R. Knauf, J.C. Lennox, J.L. Dempsey, Quantifying ligand exchange reactions at CdSe nanocrystal surfaces, *Chem. Mater.* 28 (2016) 4762–4770.
- [114] C.C. Reinhart, E. Johansson, Colloidally prepared 3-mercaptopropionic acid capped lead sulfide quantum dots, *Chem. Mater.* 27 (2015) 7313–7320.
- [115] G. Xing, N. Mathews, S. Sun, S.S. Lim, Y.M. Lam, M. Grätzel, T.C. Sum, Long-range balanced electron-and hole-transport lengths in organic-inorganic CH₃NH₃PbI₃, *Science* 342 (2013) 344–347.
- [116] G.E. Eperon, V.M. Burlakov, P. Docampo, A. Gorieli, H. Snaith, J. Morphological control for high performance, solution-processed planar heterojunction perovskite solar cells, *Adv. Funct. Mater.* 24 (2014) 151–157.
- [117] J. Feng, X. Zhu, Z. Yang, X. Zhang, J. Niu, Z. Wang, D. Yang, Record efficiency stable flexible perovskite solar cell using effective additive assistant strategy, *Adv. Math.* 30 (2018), 1801418.
- [118] P.W. Liang, C.Y. Liao, C.C. Chueh, F. Zuo, S.T. Williams, X.K. Xin, A.K.Y. Jen, Additive enhanced crystallization of solution-processed perovskite for highly efficient planar-heterojunction solar cells, *Adv. Math.* 26 (2014) 3748–3754.
- [119] T. Salim, S. Sun, Y. Abe, A. Krishna, A.C. Grimsdale, Y.M. Lam, Perovskite-based solar cells: impact of morphology and device architecture on device performance, *J. Mater. Chem. A.* 3 (2015) 8943–8969.
- [120] J. Liang, C. Wang, Y. Wang, Z. Xu, Z. Lu, Y. Ma, J. Liu, All-inorganic perovskite solar cells, *J. Am. Chem. Soc.* 138 (2016) 15829–15832.
- [121] L. Zhou, K. Yu, F. Yang, J. Zheng, Y. Zuo, C. Li, Q. Wang, All-inorganic perovskite quantum dot/mesoporous TiO₂ composite-based photodetectors with enhanced performance, *Dalton Trans.* 46 (2017) 1766–1769.
- [122] L. Zhou, K. Yu, F. Yang, H. Cong, N. Wang, J. Zheng, Q. Wang, Insight into the effect of ligand-exchange on colloidal CsPbBr₃ perovskite quantum dot/mesoporous-TiO₂ composite-based photodetectors: much faster electron injection, *Mater. Chem. C.* 5 (2017) 6224–6233.
- [123] J. Li, S.G.R. Bade, X. Shan, Z. Yu, Single-layer light-emitting diodes using organometal halide perovskite/poly(ethylene oxide) composite thin films, *Adv. Math.* 27 (2015) 5196–5202.
- [124] N. Wang, L. Cheng, R. Ge, S. Zhang, Y. Miao, W. Zou, W. Huang, Perovskite light-emitting diodes based on solution-processed self-organized multiple quantum wells, *Nat. Photonics* 10 (2016) 699.
- [125] Y.K. Chih, J.C. Wang, R.T. Yang, C.C. Liu, Y.C. Chang, Y.S. Fu, T.F. Guo, NiOx electrode interlayer and CH₃NH₂/CH₃NH₃PbBr₃ interface treatment to markedly advance hybrid perovskite-based light-emitting diodes, *Adv. Math.* 28 (2016) 8687–8694.
- [126] C.Y. Huang, C. Zou, C. Mao, K.L. Corp, Y.C. Yao, Y.J. Lee, L.Y. Lin, CsPbBr₃ perovskite quantum dot vertical cavity lasers with low threshold and high stability, *ACS Photonics* 4 (2017) 2281–2289.
- [127] S.A. Veldhuis, P.P. Boix, N. Yantara, M. Li, T.C. Sum, N. Mathews, S.G. Mhaisalkar, Perovskite materials for light-emitting diodes and lasers, *Adv. Math.* 28 (2016) 6804–6834.
- [128] A. Swarnkar, A.R. Marshall, E.M. Sanehira, B.D. Chernomordik, D.T. Moore, J.A. Christians, J.M. Luther, Quantum dot-induced phase stabilization of α -CsPbI₃ perovskite for high-efficiency photovoltaics, *Science* 354 (2016) 92–95.
- [129] M. Cha, P. Da, J. Wang, W. Wang, Z. Chen, F. Xiu, Z.S. Wang, Enhancing perovskite solar cell performance by interface engineering using CH₃NH₃PbBr_{0.9}I_{0.1} quantum dots, *J. Am. Chem. Soc.* 138 (2016) 8581–8587.
- [130] J. Han, X. Yin, H. Nan, Y. Zhou, Z. Yao, J. Li, H. Lin, Enhancing the performance of perovskite solar cells by hybridizing SnS quantum dots with CH₃NH₃PbI₃, *Small* 13 (2017), 1700953.
- [131] J. Han, S. Luo, X. Yin, Y. Zhou, H. Nan, J. Li, H. Lin, Hybrid PbS quantum-dot-in-perovskite for high-efficiency perovskite solar cell, *Small* 14 (2018), 1801016.
- [132] X. Fang, J. Ding, N. Yuan, P. Sun, M. Lv, G. Ding, C. Zhu, Graphene quantum dot incorporated perovskite films: passivating grain boundaries and facilitating electron extraction, *Phys. Chem. Chem. Phys.* 19 (2017) 6057–6063.
- [133] X.X. Liu, Z. Zhang, J. Jiang, C. Tian, X. Wang, L. Wang, C.C. Chen, Chlorine-terminated MXene quantum dots for improving crystallinity and moisture stability in high-performance perovskite solar cells, *Chem. Eng. J.* 432 (2022), 134382.
- [134] Y. Wang, A. Hu, Carbon quantum dots: synthesis, properties and applications, *J. Mater. Chem. C* 2 (2014) 6921–6939.
- [135] J. Zhang, T. Tong, L. Zhang, X. Li, H. Zou, J. Yu, Enhanced performance of planar perovskite solar cell by graphene quantum dot modification, *ACS Sustainable Chem. Eng.* 6 (2018) 8631–8640.
- [136] L. Hu, W. Wang, H. Liu, J. Peng, H. Cao, G. Shao, J. Tang, PbS colloidal quantum dots as an effective hole transporter for planar heterojunction perovskite solar cells, *J. Mater. Chem. A.* 3 (2015) 515–518.
- [137] H. Rao, W. Sun, S. Ye, W. Yan, Y. Li, H. Peng, C. Huang, Solution-processed CuS NPs as an inorganic hole-selective contact material for inverted planar perovskite solar cells, *ACS Appl. Mater. Interfaces* 8 (2016) 7800–7805.
- [138] M. Lv, J. Zhu, Y. Huang, Y. Li, Z. Shao, Y. Xu, S. Dai, Colloidal CuInS₂ quantum dots as inorganic hole-transporting material in perovskite solar cells, *ACS Appl. Mater. Interfaces* 7 (2015) 17482–17488.
- [139] W. Chen, K. Li, Y. Wang, X. Feng, Z. Liao, Q. Su, Z. He, Black phosphorus quantum dots for hole extraction of typical planar hybrid perovskite solar cells, *J. Phys. Chem. Lett.* 8 (2017) 591–598.
- [140] N. Fu, C. Huang, P. Lin, M. Zhu, T. Li, M. Ye, S. Ke, Black phosphorus quantum dots as dual-functional electron-selective materials for efficient plastic perovskite solar cells, *J. Mater. Chem. A.* 6 (2018) 8886–8894.
- [141] L. Etgar, P. Gao, P. Qin, M. Graetzel, M.K. Nazeeruddin, A hybrid lead iodide perovskite and lead sulfide QD heterojunction solar cell to obtain a panchromatic response, *J. Mater. Chem. A.* 2 (2014) 11586–11590.
- [142] Z. Yang, A. Janmohamed, X. Lan, F.P. García de Arquer, O. Voznyy, E. Yassitepe, E.H. Sargent, Colloidal quantum dot photovoltaics enhanced by perovskite shelling, *Nano Lett.* 15 (2015) 7539–7543.
- [143] Y. Li, J. Zhu, Y. Huang, J. Wei, F. Liu, Z. Shao, S. Dai, Efficient inorganic solid solar cells composed of perovskite and PbS quantum dots, *Nanoscale* 7 (2015) 9902–9907.
- [144] W.A. Dunlap-Shohl, R. Younts, B. Gautam, K. Gundogdu, D.B. Mitzi, Effects of Cd Diffusion and Doping in High-performance perovskite solar cells using CdS as electron transport layer, *J. Phys. Chem. C* 120 (2016) 16437–16445.
- [145] J. Liu, C. Gao, L. Luo, Q. Ye, X. He, L. Ouyang, W. Lau, Low-temperature solution processed metal sulfide as an electron transport layer for efficient planar perovskite solar cells, *J. Mater. Chem.* 3 (2015) 11750–11755.
- [146] Z. Gu, F. Chen, X. Zhang, Y. Liu, C. Fan, G. Wu, H. Chen, Novel planar heterostructure perovskite solar cells with CdS nanorods array as electron transport layer, *Sol. Energy Mater. Sol. Cells* 140 (2015) 396–404.
- [147] I. Hwang, K. Yong, Novel CdS hole-blocking layer for photostable perovskite solar cells, *ACS Appl. Mater. Interfaces* 8 (2016) 4226–4232.
- [148] S. Ameen, M.S. Akhtar, H.K. Seo, M.K. Nazeeruddin, H.S. Shin, An insight into atmospheric plasma jet modified ZnO quantum dots thin film for flexible perovskite solar cell: optoelectronic transient and charge trapping studies, *J. Phys. Chem. C* 119 (2015) 10379–10390.
- [149] S.S. Shin, W.S. Yang, E.J. Yeom, S.J. Lee, N.J. Jeon, Y.C. Joo, S.I. Seok, Tailoring of electron-collecting oxide nanoparticulate layer for flexible perovskite solar cells, *J. Phys. Chem. Lett.* 7 (2016) 1845–1851.
- [150] N. Sharifi, F. Tajabadi, N. Taghavinia, Recent developments in dye-sensitized solar cells, *Chem. Phys. Chem.* 15 (2014) 3902–3927.
- [151] S. Rühle, M. Shalom, A. Zaban, Quantum dot-sensitized solar cells, *Chem. Phys. Chem.* 11 (2010) 2290–2304.
- [152] M.M. Tavakoli, R. Tavakoli, Z. Nourbakhsh, A. Waleed, U.S. Virk, Z. Fan, High efficiency and stable perovskite solar cell using ZnO/rGO QDs as an electron transfer layer, *Adv. Mater. Interfac.* 3 (2016), 1500790.

- [153] Z. Yang, J. Xie, V. Arivazhagan, K. Xiao, Y. Qiang, K. Huang, D. Yang, Efficient and highly light stable planar perovskite solar cells with graphene quantum dots doped PCBM electron transport layer, *Nano Energy* 40 (2017) 345–351.
- [154] H. Zou, D. Guo, B. He, J. Yu, K. Fan, Enhanced photocurrent density of HTM-free perovskite solar cells by carbon quantum dots, *Appl. Surf. Sci.* 430 (2018) 625–631.
- [155] M.N. Lintangpradipto, N. Tsevtkov, B.C. Moon, J.K. Kang, Size-controlled CdSe quantum dots to boost light harvesting capability and stability of perovskite photovoltaic cells, *Nanoscale* 9 (2017) 10075–10083.
- [156] C. Chen, Y. Zhai, F. Li, F. Tan, G. Yue, W. Zhang, M. Wang, High efficiency $\text{CH}_3\text{NH}_3\text{PbI}_3$: CdS perovskite solar cells with CuInS_2 as the hole transporting layer, *J. Power Sources* 341 (2017) 396–403.
- [157] M. Yuan, X. Zhang, J. Kong, W. Zhou, Z. Zhou, Q. Tian, D. Kou, Controlling the band gap to improve open-circuit voltage in metal chalcogenide based perovskite solar cells, *Electrochim. Acta* 215 (2016) 374–379.
- [158] H. Li, W. Shi, W. Huang, E.P. Yao, J. Han, Z. Chen, Y. Yang, Carbon quantum dots/ TiO_x electron transport layer boosts efficiency of planar heterojunction perovskite solar cells to 19, *Nano Lett.* 17 (2017) 2328–2335.
- [159] Z. Zhu, J. Ma, Z. Wang, C. Mu, Z. Fan, L. Du, S. Yang, Efficiency enhancement of perovskite solar cells through fast electron extraction: the role of graphene quantum dots, *J. Am. Chem. Soc.* 136 (2014) 3760–3763.
- [160] Y. Tu, J. Wu, M. Zheng, J. Huo, P. Zhou, Z. Lan, M. Huang, TiO_2 quantum dots as superb compact block layers for high-performance $\text{CH}_3\text{NH}_3\text{PbI}_3$ perovskite solar cells with an efficiency of 16.97, *Nanoscale* 7 (2015) 20539–20546.
- [161] J. Ryu, J.W. Lee, H. Yu, J. Yun, K. Lee, J. Lee, J. Jang, Size effects of a graphene quantum dot modified-blocking TiO_2 layer for efficient planar perovskite solar cells, *J. Mater. Chem. A* 5 (2017) 16834–16842.
- [162] X. Zhang, Q. Wang, Z. Jin, Y. Chen, H. Liu, J. Wang, S. Liu, Graphdiyne quantum dots for much improved stability and efficiency of perovskite solar cells, *Adv. Mater. Interfac.* 5 (2018), 1701117.
- [163] M.V. Khenkin, E.A. Katz, A. Abate, G. Bardizza, J.J. Berry, C. Brabec, M. Lira-Cantu, Consensus statement for stability assessment and reporting for perovskite photovoltaics based on ISOS procedures, *Nat. Energy* 5 (2020) 35–49.
- [164] M. Cai, Y. Wu, H. Chen, X. Yang, Y. Qiang, L. Han, Cost-performance analysis of perovskite solar modules, *Adv. Sci.* 4 (2017), 1600269.
- [165] Z. Li, Y. Zhao, X. Wang, Y. Sun, Z. Zhao, Y. Li, Q. Chen, Cost analysis of perovskite tandem photovoltaics, *Joule* 2 (2018) 1559–1572.